1-1-1989

Brushless DC Synchro Drive System

K. H. Bollenbach
Purdue University

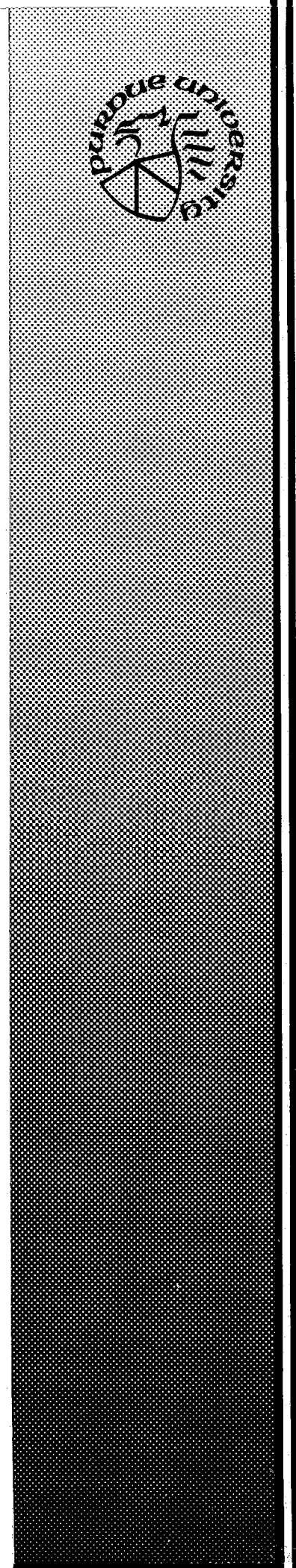

Brushless DC Synchro Drive System

K. H. Bollenbach

TR-EE 89-2
January, 1989

School of Electrical Engineering
Purdue University
West Lafayette, Indiana 47907

this is dedicated
to my parents

ACKNOWLEDGMENTS

I would like to thank Professor Wasynczuk for his tireless assistance and guidance throughout this year. Professor Krause's advice and good cheer is greatly appreciated. I would also like to thank Professor Heydt for his help in getting financial support for my research.

TABLE OF CONTENTS

Page

LIST OF TABLES

LIST OF FIGURES

Figure Page

ABSTRACT

Karl H. Bollenbach. M.S.E.E., Purdue University. December 1988. Brushless DC Synchro Drive System. Major Professor: Oleg Wasynczuk.

A brushless dc synchro drive system for use in teleoperators is investigated. The permanent-magnet synchronous machine is described and a mathematical model is presented. A dc-to-ac inverter is described and a current-band control is developed. Using the current-band inverter control system, an electromagnetic torque control scheme is developed. Through computer simulation and analysis, an operating region for this torque control method is determined. A synchro drive teleoperator system, wherein a synchronizing torque is produced electrically between the rotors of two brushless dc machines, is described which implements the previous electromagnetic torque control. A mathematical model for the teleoperator system is described and the system dynamic performance is demonstrated by computer simulation. An alternative synchro drive system configuration is also presented in which the quiescent power losses and risk of rotor demagnetization are reduced. A mathematical model is developed for this alternate configuration and a computer simulation is used to illustrate the system response.

CHAPTER 1

INTRODUCTION

A synchro drive system is a set of two or more electromechanical actuators in which the motion (generally rotational) is synchronized. For example, when there is a difference in the mechanical position between the rotors of two synchronized actuators, an electric signal is sent between the two units to maintain alignment between the rotors. Synchros have found a variety of uses in control applications. For instance, synchros can be used to maintain synchronism between a pair of mechanical shafts, to perform arithmetic operations that use angular information, or as an error detector in electric manipulators [1]. Also, synchros can be used with human interaction as a teleoperator.

A teleoperator is a synchro drive system where the response of one electric machine can be controlled by another. In the so-called master-slave configuration, a human operator guides the master unit while observing the response of a duplicate slave unit. Teleoperators are useful in that the operator can have complete control of the slave unit and while being physically separated from the slave [2].

The many applications of teleoperators are based on the need for the human operator to be removed from the hazardous environment where the slave unit is used. Teleoperator systems are used frequently when handling radioactive or other hazardous material. In a similar case, there are teleoperator uses in clean-room applications so that the operator does not contaminate a process that uses the slave unit.

The electromechanical actuators used in synchro drive systems have typically been dc machines or ac induction machines. The ac synchro drive system consists of a synchro transmitter and a synchro receiver. Both machines have a single-phase winding on the rotor and they are both connected to a common ac source. The stator of each machine has three windings with magnetic axes that are 120 ° apart. The two sets of stator windings are connected to each other. When the two rotors are in identical positions relative to their stator windings, the induced stator voltages are equal and no current flows through the windings. Thus, no electromagnetic torque is produced. If there is a difference in rotor positions between the transmitter and the receiver, the stator voltages are not equal and electric current is produced through the stator windings. In this case, a torque is produced which acts to realign the rotors [3]. In effect, the electrical connection between the transmitter and receiver causes the two rotors to act as if they are connected by a mechanical shaft.

Another electromechanical actuator used in synchro drive systems is the dc servomotor. As in the ac synchro drive system, a synchronizing torque is produced whenever there is a difference between the rotor positions of two identical dc machines. The electromagnetic torque of each dc motor is

proportional to the respective armature current which is controlled so that the torque is proportional to the measured difference in the two rotor positions. Unlike the ac synchro drive system, the dc synchro drive system can be powered by separate remotely located electric sources. Also, the connection between transmitter and receiver is a low-power electronic signal which can be transmitted, for example, by radio waves.

In this thesis, a brushless dc synchro drive system is described. Brushless dc machines have become widely used in low-power control applications. They have the advantages of having a small size, precise speed control and high reliability. In a synchro drive system, the brushless dc machines can be powered by separate electric sources and the interconnection between the two machines is a low-power electric signal. Therefore, the master and slave of the brushless dc synchro drive system can be interconnected by a radio link which is advantageous in teleoperator systems. Also, the brushless dc machine eliminates the need for mechanical commutators and brushes that are associated with conventional dc machines.

In addition to teleoperators, the brushless dc synchro drive system described in this thesis has potential automotive applications such as electronic gearing, steering, and differential drive systems. In an electric gearing system, the master unit is driven by a mechanical load. By electronic control, the speed (or position) of the slave unit can be made an integral multiple or fraction of the master unit speed (position) so that the master-slave combination possesses the salient characteristics of a mechanical gearbox. However, unlike a mechanical gearbox, there is no physical connection between the input and output shafts and the gear-ratio can be programmed electrically.

The synchro drive system can, for example, replace a steering column where the master is connected to the steering wheel and the slave would control the direction of the front wheels.

In this thesis, the individual components of the brushless dc synchro drive system are described. Then, the interconnection of the system components is set forth. The permanent-magnet synchronous machine used in this research is described and its equations are presented in Chapter 2. These equations are converted to a form which is advantageous for computer simulation. A dc-to-ac inverter used to supply the permanent-magnet synchronous machine is described in Chapter 3. In Chapter 4, the inverter-machine dynamic characteristics are investigated and a means of controlling the electromagnetic torque is described. Through computer simulation, the limitations of the drive system are then determined. In Chapter 5, the interconnection of two brushless dc motors, as part of a synchro drive system, is described. A mathematical model and its computer implementation are derived and used to demonstrate the teleoperator's response. In Chapter 6, an alternative synchro drive system configuration is introduced. A mathematical model and its implementation are also presented for this method.

CHAPTER 2

DESCRIPTION OF SYNCHRONOUS MACHINE

2.1 Introduction

The brushless dc machine considered in this thesis consists of an eight-pole two-phase permanent-magnet synchronous machine and an associated dc-to-ac inverter. In this chapter, the synchronous machine is described and a mathematical model is provided which can be used to predict its dynamic electromechanical performance.

2.2 Two-Phase Permanent-Magnet Synchronous Machine

It is convenient to describe first the electromechanical equations of a two-pole two-phase permanent-magnet synchronous machine. The resulting equations are readily modified, with a simple substitution of variables, for a P-pole machine and, in particular, for the eight-pole machine investigated.

A cross-sectional view of a two-pole two-phase synchronous machine is depicted in Fig. 2-1. As shown, there are two sets of stator windings with magnetic axes that are 90° apart. It is assumed that the resistance (and self-inductance) is the same in both stator windings. The stator voltage equations

can be expressed as

$$v_{as} = r_s\, i_{as} + p\, \lambda_{as} \tag{2.2.1}$$

$$v_{bs} = r_s\, i_{bs} + p\, \lambda_{bs} \tag{2.2.2}$$

where p is used to denote the differentiation operator d/dt. Also, λ_{as} and λ_{bs} are the flux linkages of the as- and bs-windings, respectively, and are related to the stator currents by

$$\lambda_{as} = L_{ss}\, i_{as} + \lambda'_m \sin\theta_r \tag{2.2.3}$$

$$\lambda_{bs} = L_{ss}\, i_{bs} - \lambda'_m \cos\theta_r \tag{2.2.4}$$

The second term in the right-hand side of (2.2.3) [and (2.2.4)] is the component of the stator flux linkage due to the permanent-magnet rotor. The peak magnitude of the permanent-magnet component of stator flux linkage is denoted as λ'_m. This so-called voltage constant may be established experimentally by measuring the peak open-circuit voltage while the machine is driven by a mechanical source at rated speed. In addition, θ_r is the rotor displacement defined in Fig. 2-1. Substituting (2.2.3) and (2.2.4) into (2.2.1) and (2.2.2) yields

$$v_{as} = r_s\, i_{as} + L_{ss}\, p\, i_{as} + \lambda'_m\, \omega_r \cos\theta_r \tag{2.2.5}$$

$$v_{bs} = r_s\, i_{bs} + L_{ss}\, p\, i_{bs} + \lambda'_m\, \omega_r \sin\theta_r \tag{2.2.6}$$

The previous equations may be applied to a P-pole machine if θ_r is interpreted as the "electrical" rotor displacement defined as $\theta_r = (\frac{P}{2})\, \theta_{rm}$. Here, θ_{rm} is the actual mechanical displacement and P is the number of rotor (and stator) magnetic poles. In a P-pole machine, the electromagnetic torque can be

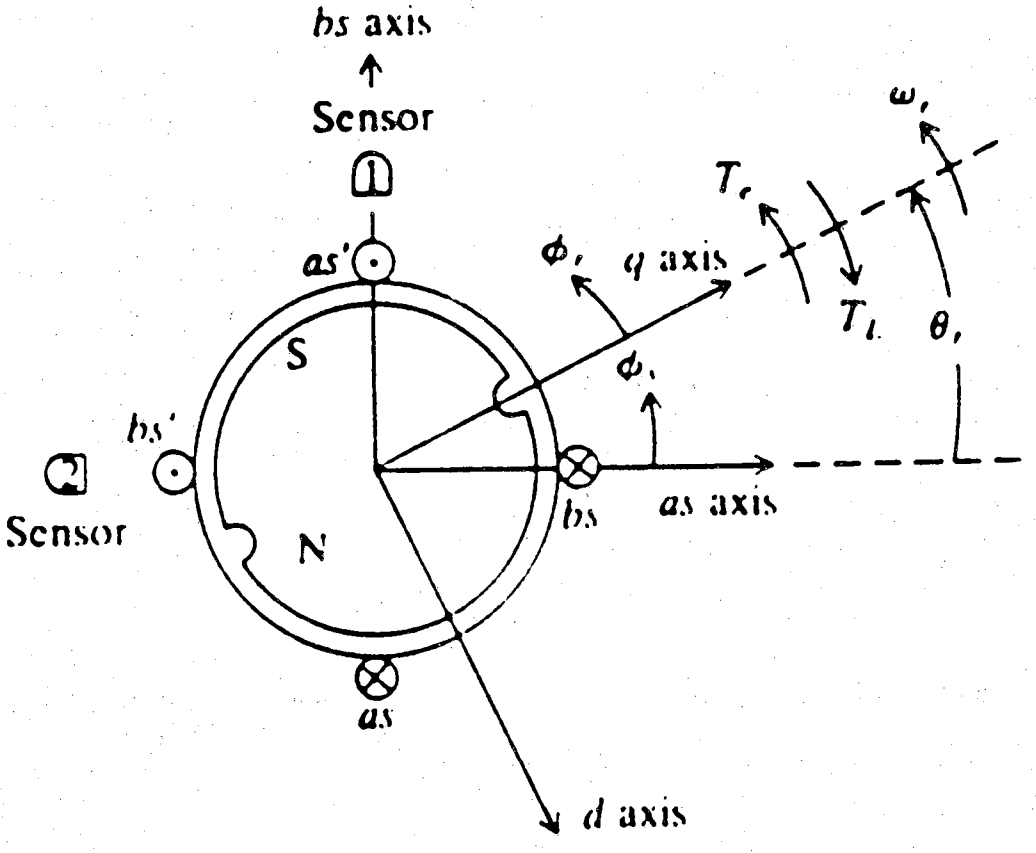

Fig. 2-1 Cross-sectional view of two-pole two-phase permanent-magnet synchronous machine.

expressed [4].

$$T_e = (\frac{P}{2}) \lambda'_m (i_{as} \cos \theta_r + i_{bs} \sin \theta_r) \quad (2.2.7)$$

The voltage and torque equations given in (2.2.5) to (2.2.7) contain coefficients which are functions of rotor position. To simplify analysis, these equations can be transformed into the rotor reference frame. The transformation of the stator variables may be expressed as

$$f^r_{qs} = f_{as} \cos \theta_r + f_{bs} \sin \theta_r \quad (2.2.8)$$

$$f^r_{ds} = f_{as} \sin \theta_r - f_{bs} \cos \theta_r \quad (2.2.9)$$

where f is a dummy variable which can represent voltage, current, or flux linkage, for example. This transformation can be viewed as a geometric projection of the as- and bs- variables onto the rotor q- and d-axis depicted in Fig. 2-1. The d-axis is defined as protruding from the north pole of the permanent-magnet rotor while the q-axis leads the d-axis by 90°. The inverse transformation is identical in form. In particular,

$$f_{as} = f^r_{qs} \cos \theta_r + f^r_{ds} \sin \theta_r \quad (2.2.10)$$

$$f_{bs} = f^r_{qs} \sin \theta_r - f^r_{ds} \cos \theta_r \quad (2.2.11)$$

By applying the change of variables to (2.2.1) through (2.2.4) and (2.2.7), the voltage and torque equations become

$$v^r_{qs} = r_s i^r_{qs} + p \lambda^r_{qs} + \omega_r \lambda^r_{ds} \quad (2.2.12)$$

$$v^r_{ds} = r_s i^r_{ds} + p \lambda^r_{ds} - \omega_r \lambda^r_{qs} \quad (2.2.13)$$

$$\lambda^r_{qs} = L_{ss}\, i^r_{qs} \tag{2.2.14}$$

$$\lambda^r_{ds} = L_{ss}\, i^r_{ds} + \lambda'_m \tag{2.2.15}$$

$$T_e = \left(\frac{P}{2}\right) \lambda'_m\, i^r_{qs} \tag{2.2.16}$$

In these equations, all coefficients are independent of the rotor position, thus simplifying analysis.

The developed electromagnetic torque can be related to the mechanical dynamics of the rotating shaft by the second-order differential equation

$$T_e = J\left(\frac{2}{P}\right) p\, \omega_r + B_m \left(\frac{2}{P}\right) \omega_r + T_L \tag{2.2.17}$$

Here, J is the inertia of the load, B_m is the damping coefficient and T_L is the applied load torque.

It is convenient to express (2.2.12) through (2.2.16) in terms of the flux linkages per second (ψ's) which are related to the flux linkages by

$$\psi = \omega_b\, \lambda \tag{2.2.18}$$

In (2.2.18), ω_b is the rated (base) electrical frequency of the rotor. Substituting (ψ/ω_b) for λ in (2.2.12) to (2.2.15) gives

$$v^r_{qs} = r_s\, i^r_{qs} + \frac{1}{\omega_b}\, p\, \psi^r_{qs} + \frac{\omega_r}{\omega_b}\, \psi^r_{ds} \tag{2.2.19}$$

$$v^r_{ds} = r_s\, i^r_{ds} + \frac{1}{\omega_b}\, p\, \psi^r_{ds} - \frac{\omega_r}{\omega_b}\, \psi^r_{qs} \tag{2.2.20}$$

where

$$\psi^r_{qs} = X_{ss}\, i^r_{qs} \tag{2.2.21}$$

$$\psi^r_{ds} = X_{ss}\, i^r_{ds} + \omega_b\, \lambda'_m \tag{2.2.22}$$

and

$$X_{ss} = \omega_b\, L_{ss} \tag{2.2.23}$$

This set of first-order differential equations can be written as

$$p\psi^r_{qs} = \omega_b \left[v^r_{qs} - r_s\, i^r_{qs} - \frac{\omega_r}{\omega_b}\, \psi^r_{ds}\right] \tag{2.2.24}$$

$$p\psi^r_{ds} = \omega_b \left[v^r_{ds} - r_s\, i^r_{ds} + \frac{\omega_r}{\omega_b}\, \psi^r_{qs}\right] \tag{2.2.25}$$

To simplify the simulation of the brushless dc machine, it is convenient to express the previous equations in per unit form. In this conversion, the variables are scaled with respect to their rated values. In particular, the equations are converted into per unit form by dividing voltages by the base voltage, currents by the base current, etc. The base (rated) voltage and current are defined at rated speed. The base impedance Z_B is defined as the ratio of base voltage to base current.

The per unit form of (2.2.24) is established by dividing both sides by the base voltage V_B.

$$\frac{p\,\psi^r_{qs}}{V_B} = \frac{\omega_b \left[v^r_{qs} - r_s\, i^r_{qs} - \dfrac{\omega_r}{\omega_b}\, \psi^r_{ds}\right]}{V_B} \tag{2.2.26}$$

Equivalently,

$$\frac{p\ \psi^r_{qs}}{V_B} = \omega_b \left[\frac{v^r_{qs}}{V_B} - \frac{r_s\ i^r_{qs}/I_B}{V_B/I_B} - \frac{\omega_r}{\omega_b}\ \frac{\psi^r_{ds}}{V_B} \right] \tag{2.2.27}$$

where I_B is the base current. The per unit variables are defined as

$$\bar{\psi}^r_{qs} = \frac{\psi^r_{qs}}{V_B} \tag{2.2.28}$$

$$\bar{i}^r_{qs} = \frac{i^r_{qs}}{I_B} \tag{2.2.29}$$

where the bar is used to distinguish per unit variables from the original variables. In terms of per unit variables, the differential equation (2.2.27) becomes

$$p\bar{\psi}^r_{qs} = \omega_b\ [\bar{v}^r_{qs} - \bar{r}_s\ \bar{i}^r_{qs} - \frac{\omega_r}{\omega_b}\ \bar{\psi}^r_{ds}] \tag{2.2.30}$$

where

$$\bar{r}_s = \frac{r_s}{V_B\ /\ I_B} = \frac{r_s}{Z_B} \tag{2.2.31}$$

Similarly,

$$p\ \bar{\psi}^r_{ds} = \omega_b\ [\bar{v}^r_{ds} - \bar{r}_s\ \bar{i}^r_{ds} + \frac{\omega_r}{\omega_b}\ \bar{\psi}^r_{qs}\ ] \tag{2.2.32}$$

Equations (2.2.21) and (2.2.22), when expressed in terms of per unit variables, become

$$\bar{\psi}^r_{qs} = \bar{X}_{ss}\ \bar{i}^r_{qs} \tag{2.2.33}$$

$$\bar{\psi}^r_{ds} = \bar{X}_{ss}\ \bar{i}^r_{ds} + \omega_r\ \bar{\lambda}'_m \tag{2.2.34}$$

where

$$\bar{X}_{ss} = \frac{\omega_b L_{ss}}{Z_B} \tag{2.2.35}$$

The per unit electromagnetic torque can be established from (2.2.16). In particular, dividing (2.2.16) by the base torque $T_B = (\frac{P}{2}) \lambda'_m I_B$ gives

$$\bar{T}_e = \frac{(\frac{P}{2}) \lambda'_m i^r_{qs}}{(\frac{P}{2}) \lambda'_m I_B} = \bar{i}^r_{qs} \tag{2.2.36}$$

It is interesting to observe that the per unit torque $\bar{T}_e$ is numerically equal to the per unit q-axis current $\bar{i}^r_{qs}$. Comparing (2.2.30) and (2.2.32) through (2.2.34) with (2.2.19) through (2.2.22) shows that the electrical equations of the synchronous machine are unchanged when expressed in per unit. However, comparing (2.2.36) with (2.2.16) reveals that the expression for electromagnetic torque is somewhat different. In particular, the factor $(\frac{P}{2}) \lambda'_m$ is absent in (2.2.36).

The mechanical dynamics, defined by (2.2.17), may be expressed in per unit by dividing both sides of (2.2.17) by the base torque $T_B = (\frac{P}{2}) \lambda'_m I_B$. After minor algebraic manipulation, the following equation results

$$\bar{T}_e = 2 H p \frac{\omega_r}{\omega_b} + D \frac{\omega_r}{\omega_b} + \bar{T}_L \tag{2.2.37}$$

where

$$H = \frac{\left(\frac{1}{2}\right)\left(\frac{2}{P}\right) J \omega_b}{T_B} \tag{2.2.38}$$

is the so-called inertia constant (typically given in seconds) and D is the damping coefficient defined as

$$D = \left(\frac{P}{2}\right) \frac{B_m \omega_b}{T_B} \tag{2.2.39}$$

The system parameters found in Table 2-1 are used in the subsequent analyses and studies. These motor parameters correspond to Magnetic Technology, Inc. Model 1600C-059-066.

Table 2-1 Electrical system data.

PARAMETER	SYMBOL	VALUE
Number of poles	P	8
Stator resistance	r_s	6.6 Ω
Stator self-inductance	L_{ss}	2.9 mH
Voltage constant	λ'_m	0.012 V·s/rad
Inertia	J	0.001 oz·in·s^2
Base electrical speed	ω_b	1608 rad/s
Base current	I_B	2.92 A
Base voltage	V_B	19.3 V
Base torque	T_B	0.140 N·m

CHAPTER 3

DESCRIPTION OF INVERTER

3.1 Introduction

In the synchro drive system described in later chapters, a dc-to-ac inverter is needed to supply current to the stator windings of each brushless dc motor. The square-wave inverter and its associated control system is described in this chapter. First, the basic layout of the inverter and its properties, assuming complementary switching, are discussed. Current-band control is introduced, which allows the inverter to reproduce an arbitrary reference waveform as a stator winding current. The operation of the square wave inverter using the current-band control method is finally described.

3.2 Square Wave Inverter

In a brushless dc drive system, the frequency of the stator variables (voltages and currents) is controlled so that it is always equal to the rotor speed. Therefore, it is necessary to have a variable-frequency ac source that can provide a current which is a function of rotor speed.

Although a linear amplifier can be used to provide the required voltages or currents, a square wave inverter is chosen, as shown in Fig 3-1, to minimize inverter power losses. The inverter consists of four transistors with the stator winding connected between the two legs of the bridge. In the two-phase machine described in the previous chapter, separate inverters are required for the two individual phases. Each switch consists of a MOSFET in parallel with a free-wheeling diode. The diode is needed to prevent the sudden interruption of current in inductive loads. Although the switching elements are depicted as MOSFETS in Fig. 3-1, other types of switching elements may be used, such as gate turn-off thyristors or bipolar transistors, depending on the power requirements. A dc source voltage is applied across the sets of series-connected switches.

In subsequent analyses, it is assumed that the transistors are switched as complementary pairs. The timing sequence in Fig 3-2 illustrates this mode of operation. When S_1 and S_4 are closed and S_2 and S_3 are open, a positive voltage is applied across v_{as}, that is, $v_{as} = + V_{dc}$. The polarity of the voltage is reversed when S_1 and and S_4 are open while S_2 and S_3 are closed, in particular $v_{as} = - V_{dc}$.

3.3 Inverter Control

The purpose of the inverter is to supply a current that closely approximates a sinusoidal reference signal. In this way, the inverter is able to control the magnitude of the stator current. In the control strategy considered, the fluctuations in current are constrained to lie within an error band around the

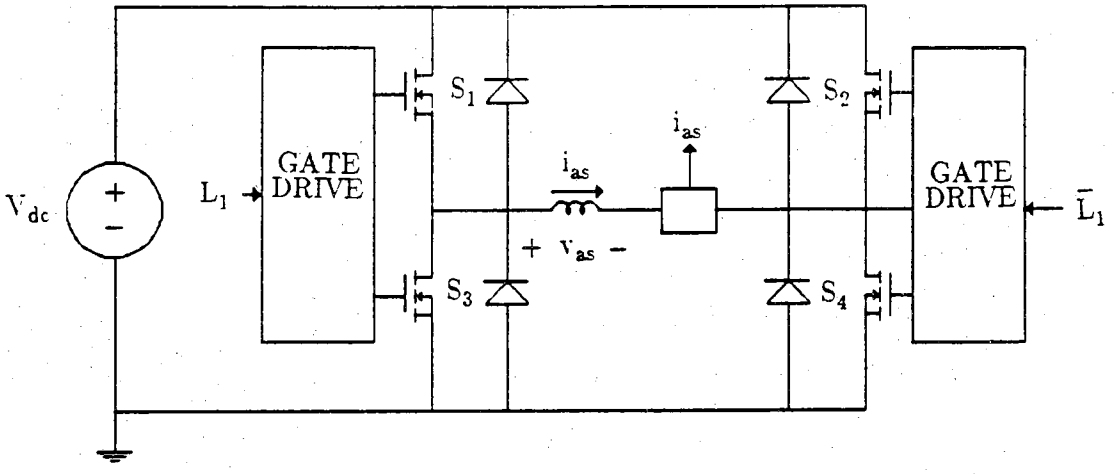

Fig. 3-1 Simplified electrical diagram of dc-to-ac inverter.

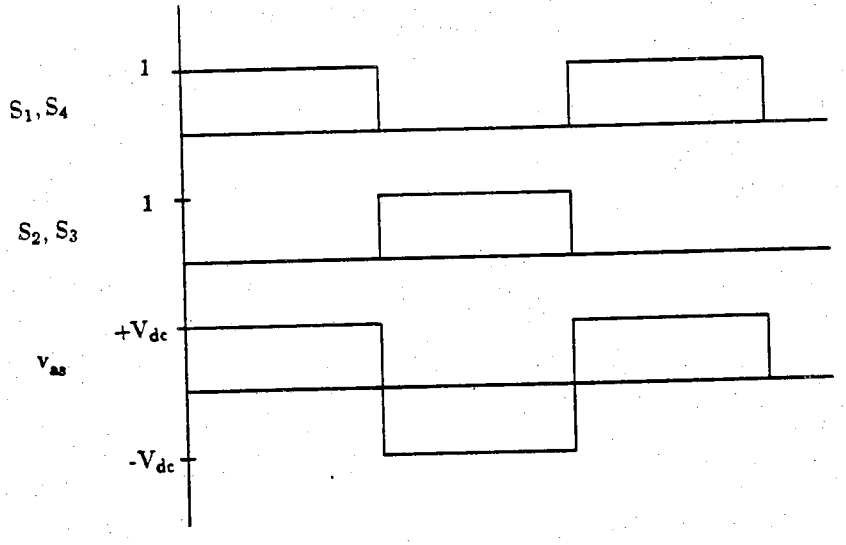

Fig. 3-2 Timing diagram.

reference. In particular, the control system switches the inverter so as to decrease the current when an upper error limit is reached and increase the current when the lower error limit is reached. This method shall be referred to as current-band control [5-6].

A hysterisis function is used to control the inverter switching as shown in Fig. 3-3. The input of this function is the difference between the reference signal i_{as}^{ref} and the measured current i_{as}. The binary output L_1 controls the gate drive signal of the MOSFETS. The two pairs of switches are never closed simultaneously; switches S_1 and S_4 are turned on when the logic signal L_1 is high while S_2 and S_3 are turned on when the complementary signal $\bar{L}_1$ is high. To prevent the possibility of short-circuiting the dc source, the driving of one pair of gates is delayed briefly until the other pair is turned off. However, this delay is brief and is neglected in subsequent analyses. When the input of the hysterisis function exceeds the $+\epsilon$ boundary, L_1 is triggered high. It remains a logic 1 until the input drops below the $-\epsilon$ boundary, whereupon L_1 returns to logic 0.

An illustration of the current following a constant reference signal is depicted in Fig. 3-4. Initially, i_{as} is assumed to be zero which is well below the negative boundary. Thus, L_1 equals logic 1, whereupon $+V_{dc}$ is applied across v_{as} and the current increases through the MOSFETS S_1 and S_4. When $i_{as}^{ref} - i_{as}$ becomes less than $-\epsilon$, L_1 is switched low, whereupon $-V_{dc}$ is applied across v_{as}, and i_{as} decreases. The current path is now through S_2 and S_3. When the lower epsilon band is reached, or $i_{as}^{ref} - i_{as} > +\epsilon$, L_1 is set high and $+V_{dc}$ is again applied to the stator winding. The switching cycle repeats itself and the current increases and decreases alternately within the epsilon error

band as shown in Fig. 3-4.

The inverter control system can likewise follow a time-varying reference signal as shown in Fig. 3-5. The error band is greatly exaggerated for illustrative purposes in both Figures 3-4 and 3-5. In practice, the error band is much smaller and i_{as} will follow, with high accuracy, the reference signal. At low input frequencies, this control can reproduce accurately a sinusoidal reference signal. However, as the frequency of the reference signal increases, there will be fewer switches per cycle and the current will become less sinusoidal (higher distortion). The performance of the control system at high frequencies will be considered in the next chapter.

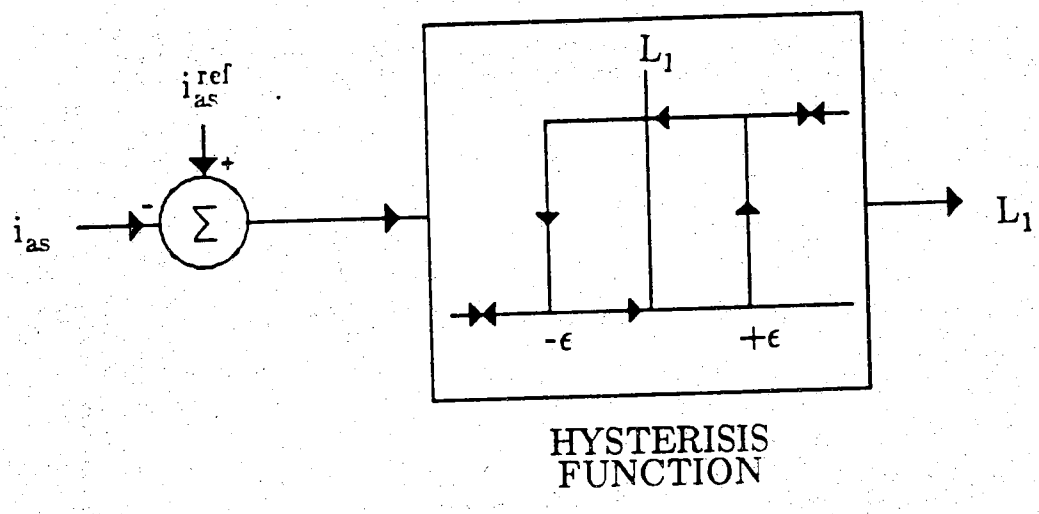

Fig. 3-3 Hysterisis function inverter control.

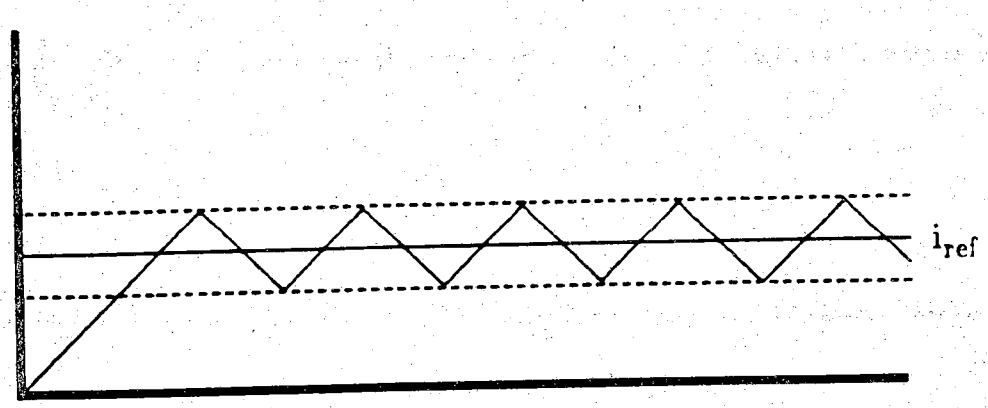

Fig. 3-4 Illustration of current-band control for constant reference current.

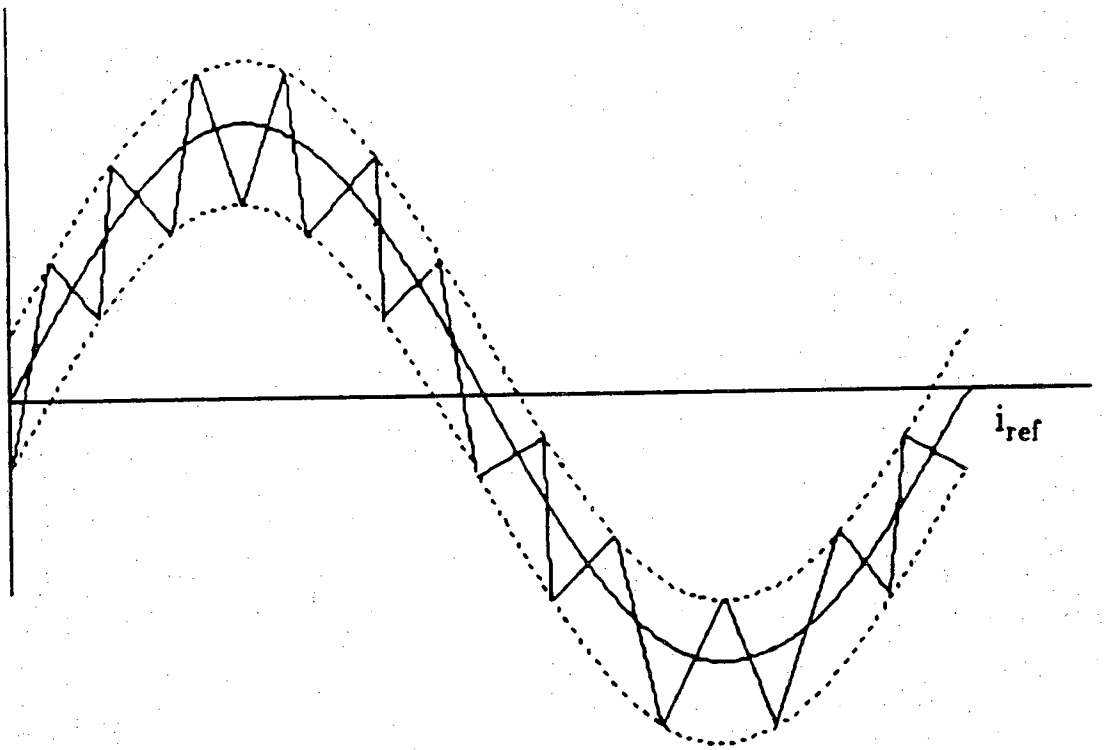

Fig. 3-5 Illustration of current-band control for sinusoidal reference current.

CHAPTER 4

TORQUE CONTROL OF BRUSHLESS DC MOTORS

4.1 Introduction

When a synchro drive system is used as a positioning device, the electromagnetic torque of the brushless dc machines must be controlled with speed and precision. In this chapter, a method of controlling the electromagnetic torque of a brushless dc machine is introduced in which the stator windings are driven by sinusoidal currents. For use in a practical system, an inverter, such as the one described in Chapter 3, is needed to supply these sinusoidal currents. A set of computer simulations at various rotor speeds illustrate the limitations of the torque control method. Finally, a mathematical model is derived which predicts an operating speed range wherein the electromagnetic torque can be controlled accurately.

4.2 Torque Control Method

In the teleoperator or electronic gearing systems described in later chapters, it is necessary to have a rapid and accurate method of controlling the electromagnetic torque. From (2.2.36), i^r_{qs} is numerically equal to T_e when

both are expressed in per unit. Thus, the electromagnetic torque can be controlled by varying the amplitude of the q-axis current. In subsequent analyses, per unit notation is assumed and bar notation is omitted for notational convenience.

The q-axis current can be related to the as- and bs-currents as

$$i_{qs}^{r} = i_{as} \cos \theta_r + i_{bs} \sin \theta_r \tag{4.2.1}$$

In order to produce a q-axis current which is independent of rotor position, the as- and bs-currents must be of the form

$$i_{as} = I_p \cos \theta_r \tag{4.2.2}$$

$$i_{bs} = I_p \sin \theta_r \tag{4.2.3}$$

Substituting (4.2.2) and (4.2.3) into (4.2.1) and simplifying,

$$i_{qs}^{r} = T_e = I_p \tag{4.2.4}$$

Thus, in order to control the electromagnetic torque of a brushless dc motor, it is necessary to supply the stator windings with currents which are sinusoidal functions of the rotor position. For the 2-phase stator currents defined by (4.2.2) and (4.2.3), the resulting electromagnetic torque is proportional to the amplitude of the stator currents.

The question arises as to whether the selected inverter, described in Chapter 3, can produce a sinusoidal current waveform of sufficient quality to control the torque. In order to evaluate the suitability of the given inverter and its associated control system, a detailed computer simulation of the brushless dc drive system was developed. In the following computer studies, it is assumed that the brushless dc motor is operating in the steady state at a

constant rotational speed.

The simulated steady-state system performance is depicted in Fig. 4-1 with a constant rotational speed of $\omega_r = 0.2\ \omega_b$ where $\omega_b = 1608$ rad/s is the base speed. In this and in subsequent studies, the following variables are plotted: the reference sinusoid (i_{as}^{ref}), the actual stator current (i_{as}), the stator voltage (v_{as}), and the electromagnetic torque (T_e). The peak amplitude of the reference current I_p is set to 1 pu in each study for purposes of comparison. In Fig. 4-1, it is seen that i_{as} has the same general shape as the reference i_{as}^{ref}. At this low speed, there are more than a hundred switches in each period of i_{as}. The stator current remains within the epsilon error band (0.10 pu) at all times. Looking closely at v_{as}, it is seen that the switching is not symmetric over a half-period. The inverter switches more frequently as the reference current approaches zero and less frequently as the reference current passes through its maximum or minimum values. Nonetheless, this has little effect on the electromagnetic torque which fluctuates about its ideal value of 1 pu. Therefore, for practical purposes, i_{as} can be considered equal to i_{as}^{ref} when $\omega_r = 0.2\ \omega_b$.

A similar study is shown in Fig. 4-2 where the rotor speed has been increased to $\omega_r = 0.8\ \omega_b$. In this case, i_{as} is not as aesthetically pleasing as in the previous study. The inverter switches less frequently at 22 times per cycle. Compared to Fig. 4-1, it is much more evident that the inverter switches less frequently as the reference current passes through zero. Here, the inverter switches only once between zero and the maximum of 1 pu as the inductive system response stays within the epsilon error band. Although this does not cause a problem at this speed, it becomes a problem at higher speeds. Torque

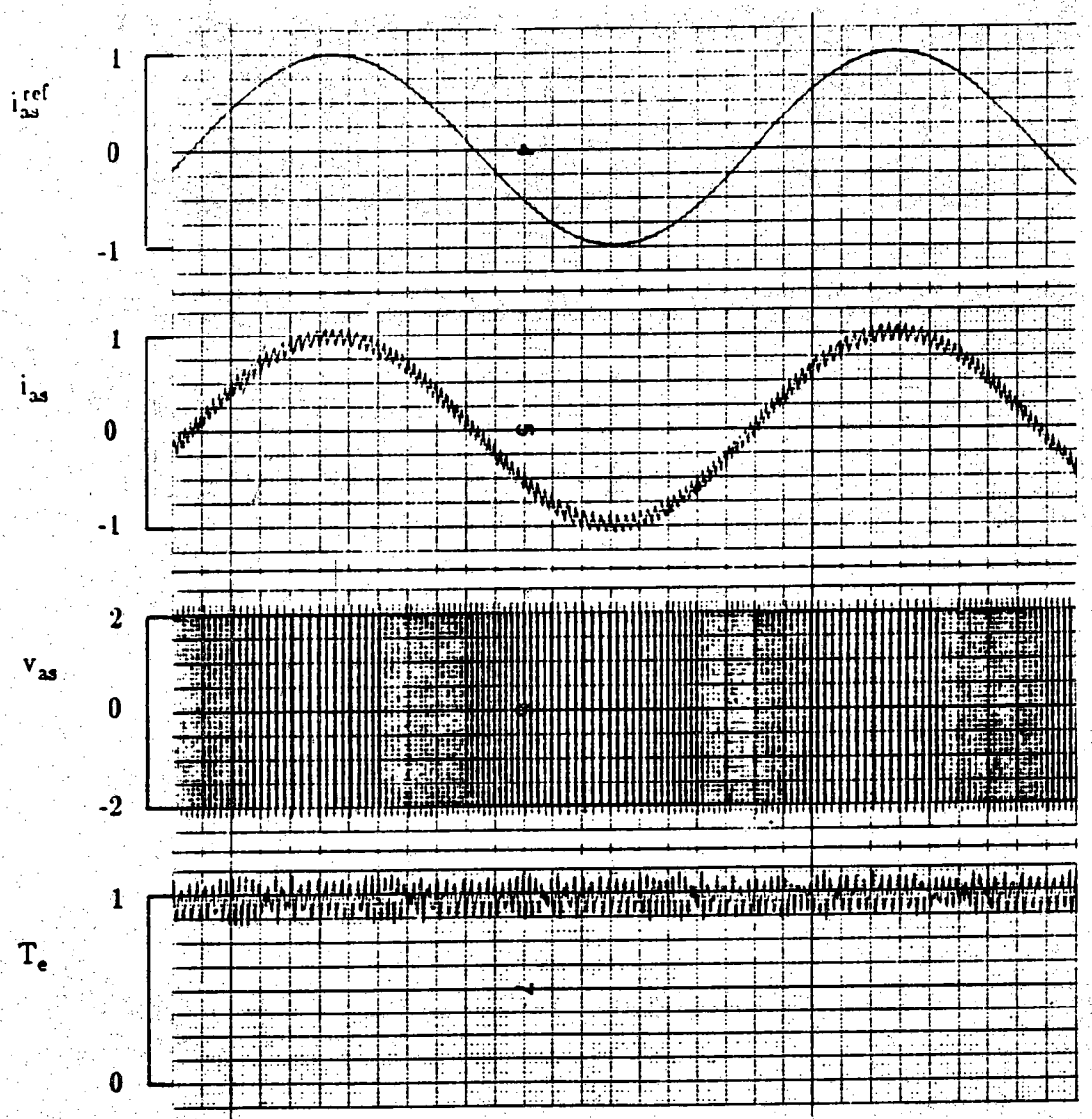

Fig. 4-1 Steady-state system performance at $\omega_r = 0.2\ \omega_b$.

is still largely unaffected by the odd shape of the waveform as its average value remains close to 1 pu. Thus, i_{as} continues to track the reference current with sufficient accuracy to produce the desired torque.

As the speed of the rotor is increased further, the current no longer tracks the reference. The steady-state performance at $\omega_r = 1.4\ \omega_b$ is shown in Fig. 4-3. The inverter now only switches six times per cycle. A difficulty occurs when the inverter switches near the zero crossing of i_{as}^{ref}. When the lower error band was reached in previous studies, the current i_{as} subsequently increased and stayed within the error band. Here, there is insufficient voltage to increase i_{as} even though the current has fallen below the lower error band. The stator current i_{as} re-enters the error band only after the peak value of i_{as}^{ref} has been passed. Thus, i_{as} reaches only 60% of its desired amplitude. The study confirms (4.2.4) where torque is equal to the amplitude of the stator currents. Torque is limited to approximately 60% of its maximum. At this speed, the desired electromagnetic torque cannot be achieved.

The steady-state response when the rotor speed is increased to $\omega_r = 1.6\ \omega_b$ is shown in Fig. 4-4. In this final study, the inverter switches only twice per cycle. The switches occur when i_{as} crosses the upper or lower error boundaries, however, the stator current fails to track the reference. Due to the inability to track the reference sinusoid, both T_e and the amplitude of i_{as} reach approximately 50% of the desired maximum. The current-band control has degenerated into a voltage control mode. It can be expected that torque will continue to drop as the rotor speed increases in this voltage mode.

The steady-state torque versus speed curve shown in Fig. 4-5 illustrates the breakdown of the torque control system. At low speeds, torque remains

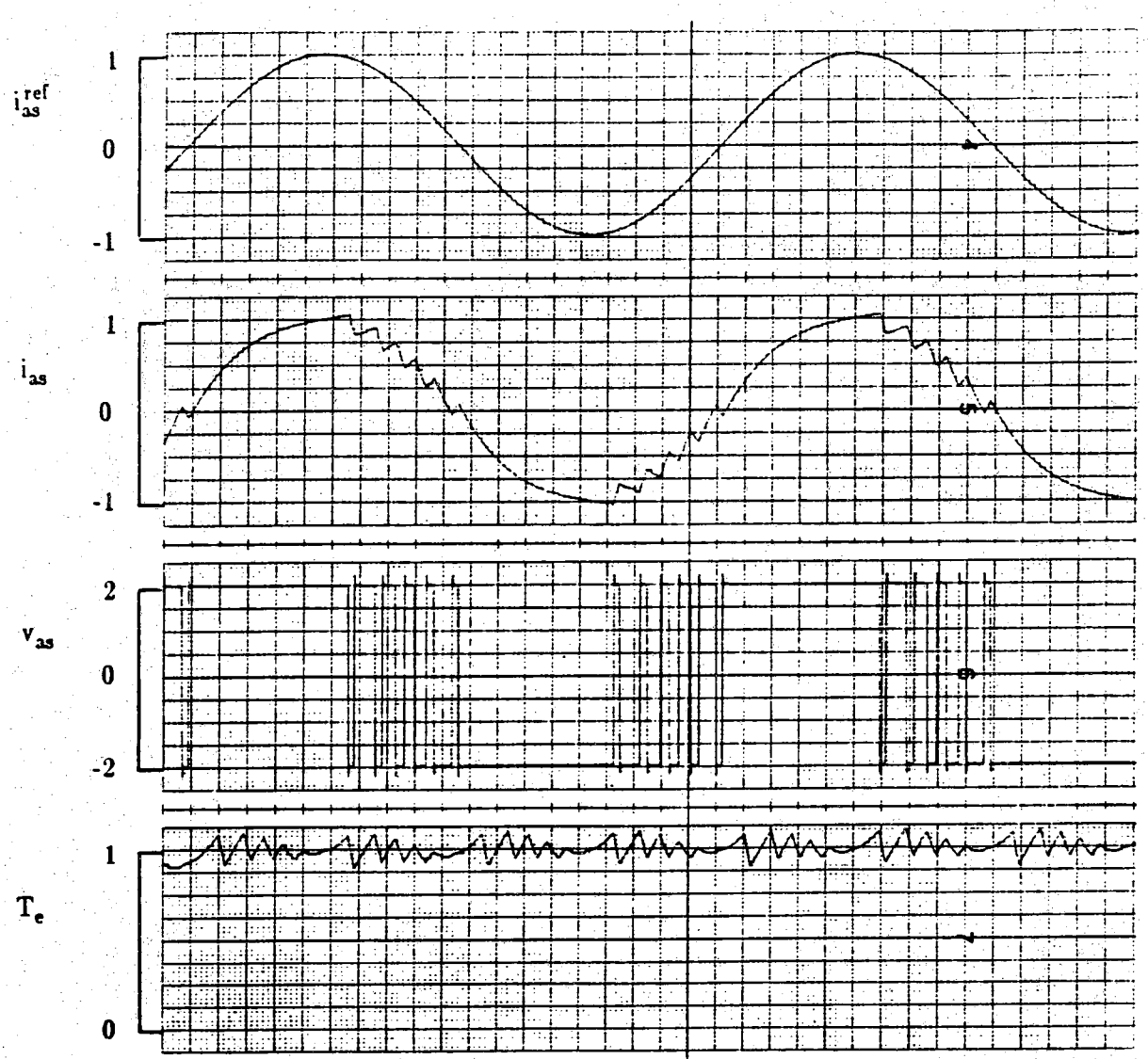

Fig. 4-2 Steady-state system performance at $\omega_r = 0.8\ \omega_b$.

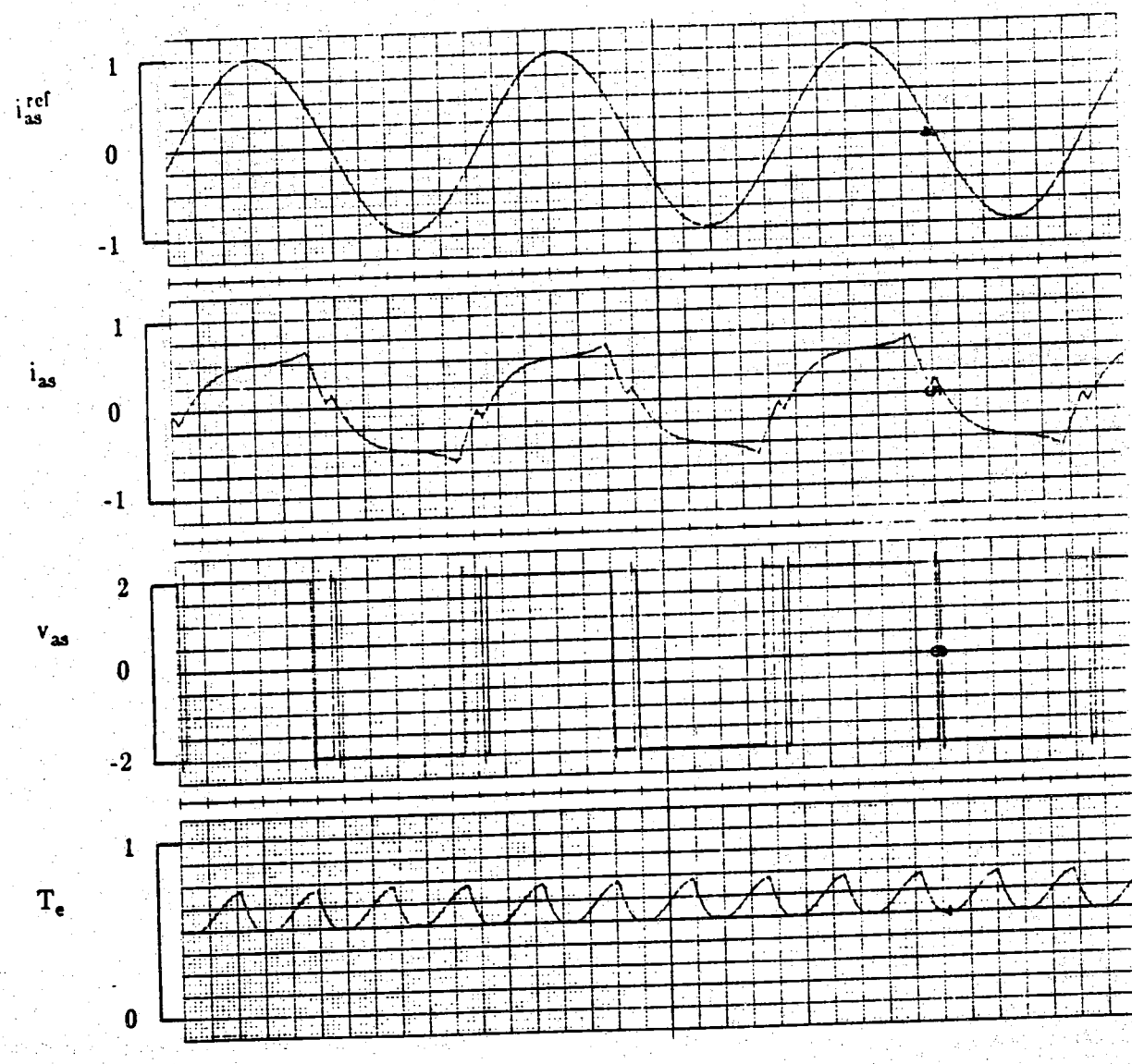

Fig. 4-3 Steady-state system performance at $\omega_r = 1.4\ \omega_b$.

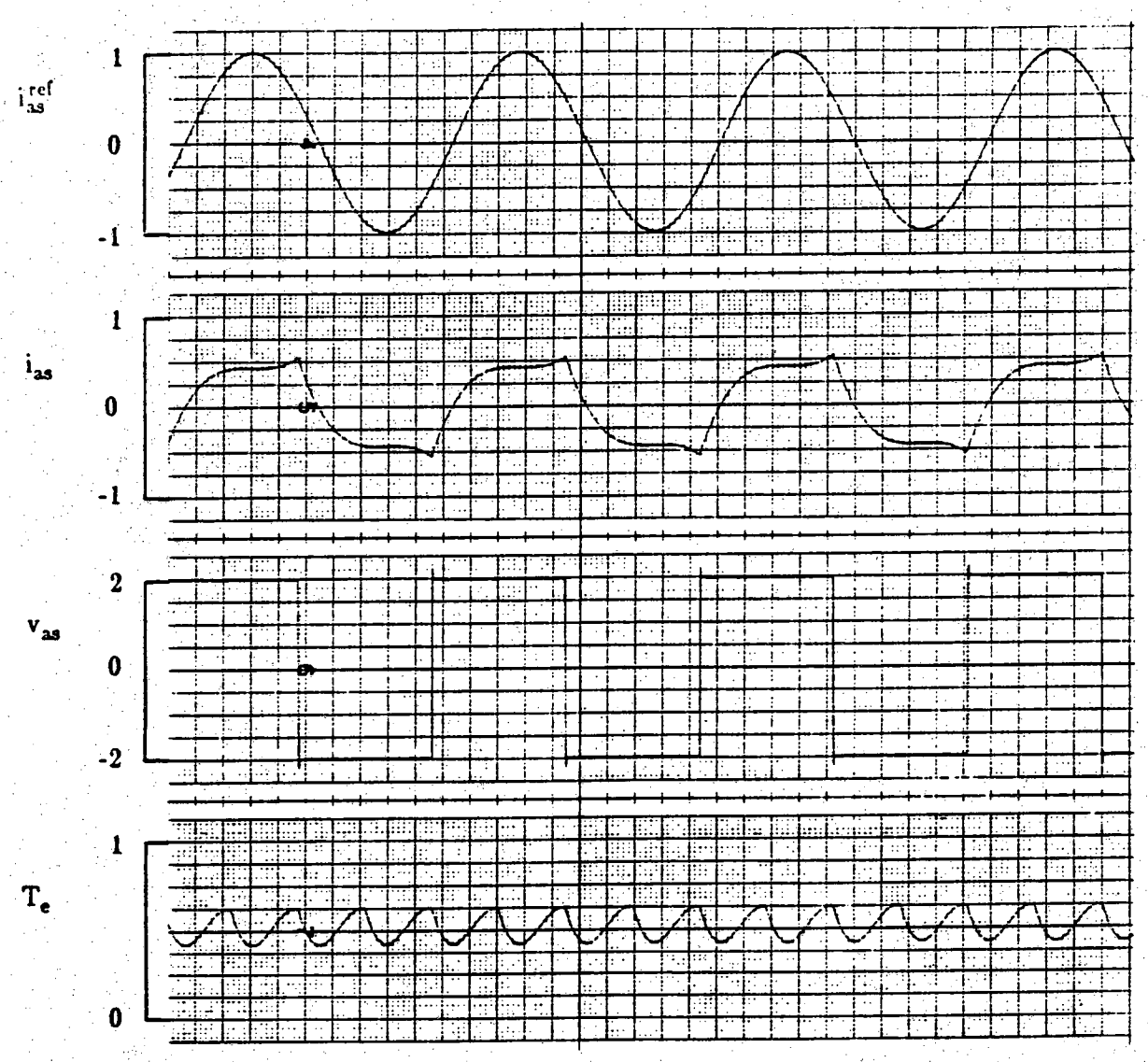

Fig. 4-4 Steady-state system performance at $\omega_r = 1.6\ \omega_b$.

constant at 1 pu. A breakpoint is reached before $\omega_r = \omega_b$ whereupon the torque begins to decrease. The torque-speed curve is somewhat linear after the breakpoint; the nonlinearities can be attributed to the change in the number of switches per cycle. It is evident that the torque is essentially constant in the low-speed region.

Figures 4-1 through 4-5 illustrate the restrictions on this method of torque control. Although the stator current tracks the reference current with high accuracy at low speeds and adequately at moderate speeds, the control system fails beyond a certain speed. It is beneficial to predict the rotor speed beyond which the current will not follow adequately the reference signal, thus limiting the torque to a value less than desired.

4.3 Determination of Torque Control Operating Region

Central to the synchro drive system considered in subsequent chapters is an accurate means of controlling the electromagnetic torque. Therefore, it becomes important to predict the rotor speed range in which the stator currents will track the reference currents without exceeding the epsilon error band, thus producing the desired torque.

The failure to track the reference currents occurs when, due to the back emf of the brushless dc motor, the current fails to increase even though positive source voltage is applied to the winding (equivalently, when the current fails to decrease when a negative source voltage is applied). The speed range for which tracking is guaranteed may be established by comparing the rate of change of stator current, with positive applied voltage, to the rate of change

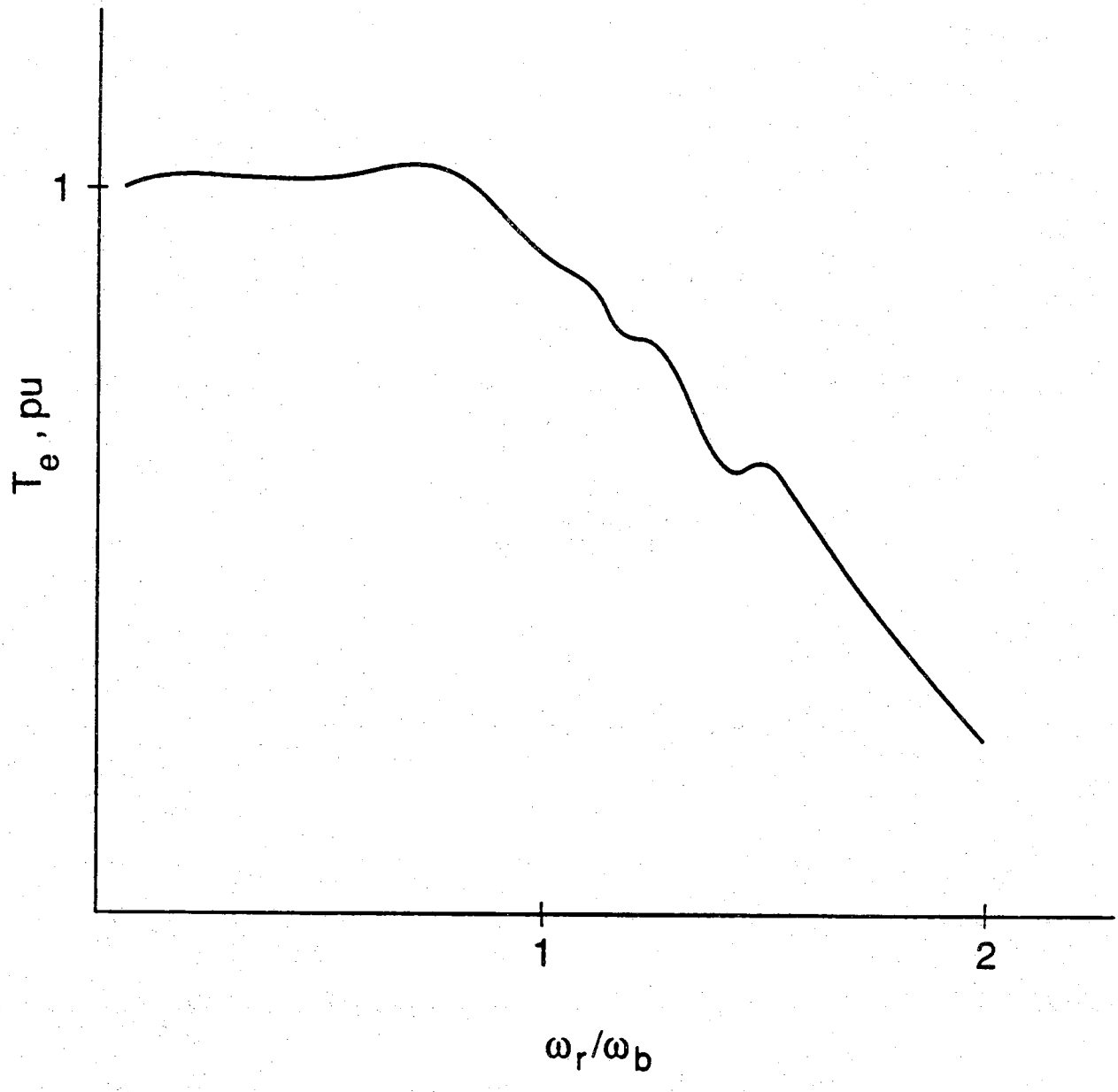

Fig. 4-5 Steady-state torque versus speed.

of reference current. To ensure tracking, it is necessary that

$$p\, i_{as} > p\, i_{as}^{ref} \text{ when } v_{as} = +V_{dc} \tag{4.3.1}$$

and

$$p\, i_{as} < p\, i_{as}^{ref} \text{ when } v_{as} = -V_{dc} \tag{4.3.2}$$

In either case, it is assumed that

$$i_{as}^{ref} = \sqrt{2}\, I_s \cos \theta_r \tag{4.3.3}$$

Differentiating,

$$p\, i_{as}^{ref} = -\sqrt{2}\, I_s\, \omega_r \sin \theta_r \tag{4.3.4}$$

From (2.2.5) with $v_{as} = +V_{dc}$,

$$p\, i_{as} = \frac{1}{L_{ss}} [V_{dc} - r_s\, i_{as} - \omega_r\, \lambda'_m \cos \theta_r] \tag{4.3.5}$$

From (4.3.1)

$$p\, i_{as} - p\, i_{as}^{ref} > 0 \text{ when } v_{as} = +V_{dc} \tag{4.3.6}$$

Substituting (4.3.4) and (4.3.5) into (4.3.6),

$$\frac{1}{L_{ss}} [V_{dc} - r_s\, i_{as} - \omega_r\, \lambda'_m \cos \theta_r] + \sqrt{2}\, I_s\, \omega_r \sin \theta_r > 0 \tag{4.3.7}$$

Equivalently

$$V_{dc} > r_s\, i_{as} + \omega_r\, \lambda'_m \cos\theta_r - \sqrt{2}\, I_s\, L_{ss}\, \omega_r \sin\theta_r \tag{4.3.8}$$

Assuming that i_{as} is approximately equal to the reference i_{as}^{ref} when it is within the error band,

$$i_{as} \simeq \sqrt{2}\, I_s \cos \theta_r \tag{4.3.9}$$

whereupon (4.3-8) becomes

$$V_{dc} > (\sqrt{2}\ r_s\ I_s + \omega_r\ \lambda'_m)\cos\theta_r - \sqrt{2}\ I_s\ L_{ss}\ \omega_r \sin\theta_r \qquad (4.3.10)$$

Equivalently

$$V_{dc} > \cos(\theta_r + \phi)\left[(\sqrt{2}\ r_s\ I_s + \frac{\omega_r}{\omega_b}\lambda'_m\ \omega_b)^2 + (\sqrt{2}\ I_s\ X_{ss}\ \frac{\omega_r}{\omega_b})^2\right]^{1/2}$$

(4.3.11)

where

$$\phi = \tan^{-1}\frac{\sqrt{2}\ I_s\ L_{ss}\ \omega_r}{\sqrt{2}\ r_s\ I_s + \omega_r\ \lambda'_m} \qquad (4.3.12)$$

The previous inequality should be satisfied for all values of θ_r whereupon

$$V_{dc} > \left[(\sqrt{2}\ r_s\ I_s + \frac{\omega_r}{\omega_b}\lambda'_m\ \omega_b)^2 + (\sqrt{2}\ I_s\ X_{ss}\ \frac{\omega_r}{\omega_b})^2\right]^{1/2} \qquad (4.3.13)$$

Solving for $\frac{\omega_r}{\omega_b}$, a quadratic inequality results.

$$0 > ((\lambda'_m)^2\ \omega_b^2 + 2\ I_s^2\ X_{ss}^2)\left(\frac{\omega_r}{\omega_b}\right)^2 + 2\sqrt{2}\ r_s\ I_s\left(\frac{\omega_r}{\omega_b}\right) + (2\ r_s^2\ I_s^2 - V_{dc}^2)$$

(4.3.14)

The maximum speed for which this equality is satisfied is

$$\left(\frac{\omega_r}{\omega_b}\right)_{bp} = \frac{-2\sqrt{2}\ r_s\ I_s + \sqrt{(2\sqrt{2}\ r_s\ I_s)^2 - 4\ [(\lambda'_m\ \omega_b)^2 + 2\ I_s^2\ X_{ss}^2](2\ r_s^2\ I_s^2 - V_{dc}^2)}}{2\ [(\lambda'_m\ \omega_b)^2 + 2\ I_s^2\ X_{ss}^2]}$$

(4.3.15)

Below this speed, tracking is guaranteed and the electromagnetic torque can be controlled with high accuracy. Beyond this speed, the torque is reduced due to the inability to supply the desired reference currents. For the machine parameters given in Chapter 2, the calculated maximum speed below which tracking is guaranteed is $\left(\frac{\omega_r}{\omega_b}\right)_{bp} = 0.728$. This compares favorably with the breakpoint value depicted in Fig. 4-5.

CHAPTER 5

BRUSHLESS SYNCHRO DRIVE SYSTEM

5.1 Introduction

A synchro drive control method is proposed in this chapter. A master-slave control system that uses sinusoidal input currents to control the torque of two identical brushless dc machines is described. The implementation of this method of control is explained at the system level and a simplified mathematical model of the synchro drive system is developed which can be used to predict its electromechanical behavior. A computer simulation is performed to compare the practical characteristics of the control system to that of the simplified model.

5.2 Control Scheme Derivation

The primary objective of the synchro drive system is to have one brushless dc motor follow the other mechanically. In other words, the two motors should respond as if they were connected by a mechanical shaft. In subsequent discussions, it is convenient to refer to one of the motors as the master and the other as the slave unit in a master-slave combination.

The torque applied to the rotor of the master by a fictitious mechanical shaft connecting the master and slave can be written as

$$T_1 = K(\theta_{r2} - \theta_{r1}) \tag{5.2.1}$$

where K is the stiffness constant of the shaft, θ_{r1} is the position of the master, and θ_{r2} is the position of the slave. An equal and opposite torque is applied to the slave, i.e.

$$T_2 = K(\theta_{r1} - \theta_{r2}) \tag{5.2.2}$$

In the synchro drive control system, an electromagnetic torque is produced which is proportional to the sine of the difference between the two rotor positions. Assuming an ideal sinusoidal output from the inverter, the stator currents of the master may be expressed

$$i_{as1} = I_p \sin \theta_{r2} \tag{5.2.3}$$

$$i_{bs1} = -I_p \cos \theta_{r2} \tag{5.2.4}$$

where I_p is constant. Likewise the stator currents of the slave are

$$i_{as2} = I_p \sin \theta_{r1} \tag{5.2.5}$$

$$i_{bs2} = -I_p \cos \theta_{r1} \tag{5.2.6}$$

It is important to note that the stator currents of the master are proportional to the sine and cosine of the slave unit position and vice versa. The stator currents of the master can be transformed to the rotor reference frame using (2.2.8) and (2.2.9).

$$i_{qs1}^{r1} = I_p \sin(\theta_{r2} - \theta_{r1}) \tag{5.2.7}$$

$$i_{ds1}^{r1} = I_p \cos(\theta_{r2} - \theta_{r1}) \tag{5.2.8}$$

where the superscript r1 denotes the rotor reference frame of the master. Applying the same transformation to the slave results in

$$i_{qs2}^{r2} = I_p \sin(\theta_{r1} - \theta_{r2}) \tag{5.2.9}$$

$$i_{ds2}^{r2} = I_p \cos(\theta_{r1} - \theta_{r2}) \tag{5.2.10}$$

Since T_e is equal to i_{qs}^{r} in per unit,

$$T_{e1} = i_{qs1}^{r1} = I_p \sin(\theta_{r2} - \theta_{r1}) \tag{5.2.11}$$

and

$$T_{e2} = i_{qs2}^{r2} = I_p \sin(\theta_{r1} - \theta_{r2}) \tag{5.2.12}$$

If the displacement between rotors is small, the torque will be approximately linearly related to the difference in positions. That is, if $\theta_{r1} \simeq \theta_{r2}$, then

$$T_{e1} \simeq I_p (\theta_{r2} - \theta_{r1}) \tag{5.2.13}$$

and

$$T_{e2} \simeq I_p (\theta_{r1} - \theta_{r2}) \tag{5.2.14}$$

These equations are identical to the mechanical relationships of (5.2.1) and (5.2.2), where the stiffness constant is equal to the amplitude of the stator currents.

5.3 System Level Control

In this section, a system-level control is described which applies the equations of the previous section. The expressions for electromagnetic torque, as given in (5.2.11) and (5.2.12), are valid only if the stator currents i_{as} and i_{bs} are ideal sinusoids. Although the inverter output currents will not be ideal sinusoids, the inverter can produce sinusoids of sufficient accuracy within a given rotor speed range, as seen in the computer studies of the previous chapter. The sinusoidal reference current can be synthesized from discrete position information established from an optical encoder. It is assumed in the following discussions that the reference sinusoids may be considered as ideal. The resolution of the position encoder must be sufficiently high to meet this requirement. Here, the layout of the following system and its implementation is explained so that, for all practical purposes, the electromagnetic torque may be considered as ideal.

This method of controlling two brushless dc machines, where one follows the other in a master-slave configuration, is shown in Fig. 5-1. Although only the control system of the master is shown, the slave control is identical. Only the subscripts of θ_{r1} and θ_{r2} need to be interchanged for the slave control. Here, digital measurements from the optical position encoders are exchanged between the two motor controls. These received digital positions are converted into continuous (analog) reference signals used to drive the inverters.

The inverter blocks consist of two single-phase dc-to-ac inverters as in Figures 3-1 and 3-3. The stator windings in Fig 5-1 are depicted as inductors. The single inputs to the inverters are the sinusoidal reference signals defined in (5.2.3) and (5.2.4). The outputs of the blocks are the winding currents.

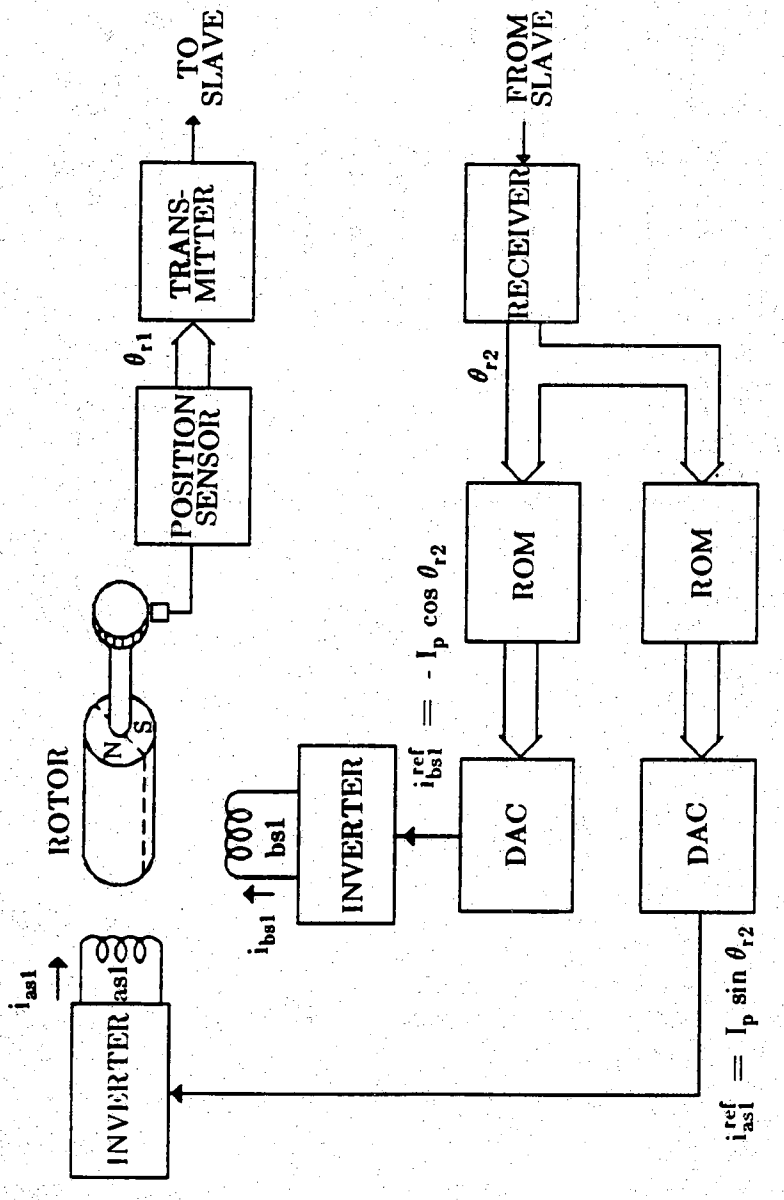

Fig. 5-1 System-level control.

Since the currents that drive the master are functions of θ_{r2}, this position must be measured by the slave control and sent to the master. In other words, position information is exchanged between the two motors. The position can be sensed optically (optical encoder), magnetically (Hall effect devices) or through buried sensor windings. The main requirement of the sensor is that its resolution must be sufficiently high that it can be considered as an analog signal. In Fig. 5-1, the output of the position sensor is depicted as a binary signal. This information is sent by the transmitter in a serial form to the receiver of the slave machine. Transmission can be done electrically or by a radio link. In turn, the master receives position information from the slave.

The two reference sinusoidal waveforms used by the inverters are derived from the incoming position information. The binary output of the receiver defines the address of a set of read only memory (ROM) integrated circuits which store, in binary form, the sine and cosine of the input angle. Once again, these discrete sinusoidal functions must be of sufficient precision so that when they are converted to analog form, low-distortion sinusoids are produced. The outputs of the ROM look-up table are converted to analog reference signals using digital-to-analog converters (DACS) which, in turn, define the input reference currents supplied to the inverter control system.

5.4 Computer Analysis

A computer study and analysis is performed to investigate the performance of the control system described in the previous section. The mechanical system response of the slave motor is depicted in Fig. 5-2 for a step change in the position of the master θ_{r1}. It is assumed in this and in subsequent studies that the position measurement system and the analog conversion are precise enough so that the reference can be considered as ideal. The following variables are plotted in Fig. 5-2: the stator currents of the slave (i_{as2} and i_{bs2}), the rotor reference frame currents of the slave (i_{qs2}^{r2} and i_{ds2}^{r2}), the angular positions of the master and slave (θ_{r1} and θ_{r2}), and the speed of the slave (ω_{r2}/ω_b). The peak current (stiffness constant) I_p is set to 1 pu in each study for purposes of comparison.

Referring to Fig. 5-2, both rotors begin at rest as $\theta_{r1} = \theta_{r2} = 0$. The master position θ_{r1} is the reference position supplied to the slave and is stepped from 0 ° to 60 °. The peak value of θ_{r2} is equal to twice the magnitude of the step change in θ_{r1}. The frequency of the ensuing oscillations of θ_{r2} is found to be approximately 278 rad/sec and the time-constant associated with the decay of these oscillations is 0.73 s.

Each of the plotted currents match the predicted results of (5.2.3), (5.2.4), (5.2.7) and (5.2.8). Since i_{as2} and i_{bs2} are sinusoidal functions of the stepped angle θ_{r1}, they are also step functions. After the step change in θ_{r1}, $i_{as2} = \sin 60° = 0.866$ and $i_{bs2} = -\cos 60° = -0.5$. The rotor reference frame currents i_{qs2}^{r2} and i_{ds2}^{r2} oscillate because they are functions of the difference in rotor positions. The current i_{qs2}^{r2} appears to oscillate at the same frequency as θ_{r2} while i_{ds2}^{r2} oscillates at twice the frequency of θ_{r1} because it

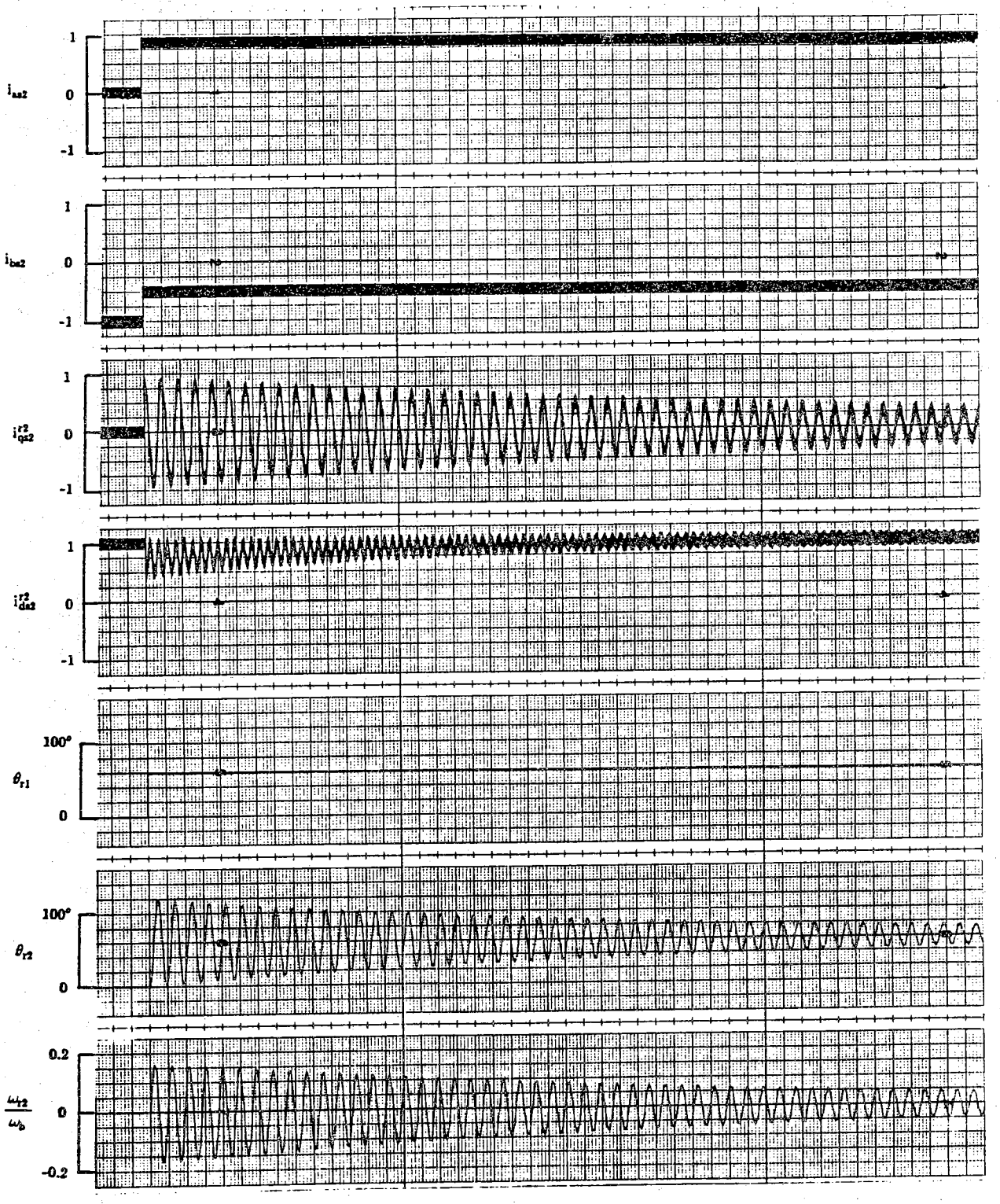

Fig. 5-2 Slave unit response for step change in master position.

varies about cos 0°. Since θ_{r1} initially deviates 60° from its desired position, i_{qs2}^{r2} varies a maximum of sin 60° = 0.866 and i_{ds2}^{r2} drops as low as cos 60° = 0.5. As θ_{r2} approaches θ_{r1}, i_{qs2}^{r2} and i_{ds2}^{r2} damp back to their original values of 0 pu and 1 pu, respectively, with the same exponential decay time-constant as θ_{r2}.

The damping time-constant and oscillation frequency of the electrical torque can be approximated to confirm the mechanics of the computer study. The mechanical equation in per unit form is,

$$T_{e2} = T_L + 2\,H\,p\,\frac{\omega_{r2}}{\omega_b} + D\,\frac{\omega_{r2}}{\omega_b} \tag{5.4.1}$$

From (5.2.12), the electromagnetic torque of the slave is

$$T_{e2} = I_p \sin(\theta_{r1} - \theta_{r2}) \tag{5.4.2}$$

To simplify the analysis, I_p is set at 1 pu and it will be assumed that sin $(\theta_{r1} - \theta_{r2}) \simeq (\theta_{r1} - \theta_{r2})$. The latter is true for small changes in position. After setting $T_L = 0$, and since $\omega_r = p\theta_r$, the mechanical equation becomes

$$(\theta_{r1} - \theta_{r2}) = \frac{2\,H}{\omega_b}\,p^2\,\theta_{r2} + \frac{D}{\omega_b}\,p\,\theta_{r2} \tag{5.4.3}$$

Equivalently,

$$\frac{\omega_b}{2\,H}\,\theta_{r1} = p^2\,\theta_{r2} + \frac{D}{2\,H}\,p\,\theta_{r2} + \frac{\omega_b}{2\,H}\,\theta_{r2} \tag{5.4.4}$$

Converting to state model form yields [7],

$$p\begin{bmatrix}\theta_{r2}\\ \omega_{r2}\end{bmatrix} = \begin{bmatrix}\dfrac{-D}{2H} & 1\\ -\dfrac{\omega_b}{2H} & 0\end{bmatrix}\begin{bmatrix}\theta_{r2}\\ \omega_{r2}\end{bmatrix} + \begin{bmatrix}0\\ \dfrac{\omega_b}{2H}\end{bmatrix}\theta_{r1} \tag{5.4.5}$$

Using the parameters H = 0.01 s, D = 0.05 and ω_b = 1608 rad/sec, the state equations become

$$p\begin{bmatrix}\theta_{r2}\\ \omega_{r2}\end{bmatrix} = \begin{bmatrix}-2.5 & 1\\ -80400 & 0\end{bmatrix}\begin{bmatrix}\theta_{r2}\\ \omega_{r2}\end{bmatrix} + \begin{bmatrix}0\\ -80400\end{bmatrix}\theta_{r1} \tag{5.4.6}$$

The eigenvalues of the state matrix are

$$\lambda_1 = -1.25 - j283.5, \qquad \lambda_2 = -1.25 + j283.5 \tag{5.4.7}$$

The imaginary part of the eigenvalue corresponds to the natural frequency of oscillation while the reciprocal of the real part is the time-constant associated with the exponential decay. In particular,

$$\tau = 0.8 \text{ s} \qquad \omega_n = 283.5 \text{ rad/s} \tag{5.4.8}$$

These results compare favorably with the results depicted in Fig. 5-2. The variations in the two sets of results are due to the error in the previous graphical approximations. The simulation thereby confirms the practical results of the teleoperator control system.

The computer study in Fig. 5-2 illustrates several disadvantages of the system control. First, the amplitude of the stator current is constant and equal to the rated value during steady-state operation regardless of the mechanical load. Consequently, there is a constant, quiescent loss of power in the stator windings, regardless of the rotor position or mechanical load. In particular,

$$P_{losses} = r_s \left(i_{as}^2 + i_{bs}^2 \right)$$

$$= r_s \left(I_p^2 \sin^2 \theta_r + I_p^2 \cos^2 \theta_r \right)$$

$$= r_s I_p^2 \qquad (5.4.9)$$

This power will be dissipated in the stator windings regardless of whether the machine is in motion or at rest. A second disadvantage of this method of control is that a large d-axis current at no-load conditions may lead to demagnetization of the rotor permanent magnets.

CHAPTER 6

AMPLITUDE-MODULATED SYNCHRO DRIVE SYSTEM

6.1 Introduction

The teleoperator control system described in Chapter 5 offers precise and fast position control. However, there are potential disadvantages with this system such as rotor demagnetization and substantial quiescent stator power losses. In this chapter, an alternative synchro drive system is described in which the electromechanical torque is controlled by varying the amplitude of the stator currents. A computer study is then performed to illustrate the mechanical and electrical response of this teleoperator control system.

6.2 Control Scheme Derivation

In this section, a control approach is described which eliminates quiescent stator power losses and reduces the possibility of rotor demagnetization. Since a large d-axis current can demagnetize the rotor, it is advantageous to set i^r_{ds} equal to zero. In this case, the q-axis current i^r_{qs} will be proportional to the stator current magnitude. Thus, the electromagnetic torque can be controlled linearly through the magnitude of the stator currents. Referring to (2.2.9),

$$i_{ds}^{r1} = i_{as1} \sin \theta_{r1} - i_{bs1} \cos \theta_{r1} \tag{6.2.1}$$

Setting i_{ds}^{r1} to zero yields

$$i_{as1} \sin \theta_{r1} = i_{bs1} \cos \theta_{r1} \tag{6.2.2}$$

Likewise, for the slave

$$i_{as2} \sin \theta_{r2} = i_{bs2} \cos \theta_{r2} \tag{6.2.3}$$

By satisfying (6.2.2) and (6.2.3), the d-axis current will remain equal to zero for all time and the risk of rotor demagnetization is reduced. The stator currents of the master are again set as sinusoidal waveforms

$$i_{as1} = I_{p1} \cos \theta_{r1} \tag{6.2.4}$$

$$i_{bs1} = I_{p1} \sin \theta_{r1} \tag{6.2.5}$$

To satisfy the equality in (6.2.3), the slave currents are expressed as

$$i_{as2} = I_{p2} \cos \theta_{r2} \tag{6.2.6}$$

$$i_{bs2} = I_{p2} \sin \theta_{r2} \tag{6.2.7}$$

where I_{p1} and I_{p2} are controllable variables. It is noted that (6.2.4) through (6.2.7) are identical in form to the torque control in (4.2.2) and (4.2.3). The stator currents of the master are transformed to the rotor reference frame using (2.2.8) and (2.2.9).

$$i_{qs1}^{r1} = I_{p1} \tag{6.2.8}$$

$$i_{ds1}^{r1} = 0 \tag{6.2.9}$$

Applying the same transformation to the slave results in

$$i_{qs2}^{r2} = I_{p2} \tag{6.2.10}$$

$$i_{ds2}^{r2} = 0 \tag{6.2.11}$$

As shown in (2.2.36), T_e is equal to i_{qs}^{r} in per unit. Thus

$$T_{e1} = I_{p1} \tag{6.2.12}$$

$$T_{e2} = I_{p2} \tag{6.2.13}$$

An identical result for torque is found in (4.2.4). Electromagnetic torque is controlled by varying the amplitude of the stator currents. In order to produce a torque which aligns the rotors of the synchro master and slave, the current amplitudes are controlled so that

$$T_{e1} = I_{p1} = K(\theta_{r2} - \theta_{r1}) \tag{6.2.14}$$

$$T_{e2} = I_{p2} = K(\theta_{r1} - \theta_{r2}) \tag{6.2.15}$$

where K is the stiffness constant of the shaft.

Comparing (6.2.14) and (6.2.15) to (5.2.13) and (5.2.14), the mechanical equations of the amplitude-modulated system are identical to those of the constant-current method, while the limitations of the constant-current system are avoided. When $\theta_{r1} = \theta_{r2}$, the amplitude of the stator currents are zero. Therefore, there are no quiescent power losses when the teleoperator is at rest. Also, since the d-axis current in both the master and slave are zero, the possibility of rotor demagnetization is significantly reduced.

6.3 System Control Layout

The current and electromagnetic torque relations of the previous section can be implemented with the control system shown in Fig. 6-1 which corresponds to the master. The control system for the slave unit is identical with θ_{r1} and θ_{r2} interchanged. All assumptions made in Section 5.3 concerning the precision of the binary position information and the reference sinusoids are assumed to apply herein.

Although the basic layout is the same as in the previous chapter, there are some differences in the system components. First, the output of the ROM sinusoid look-up table is a function of the master position θ_{r1} rather than of the slave position θ_{r2}. A multiplying digital to analog converter (MDAC) is necessary to produce a variable-amplitude reference sinusoid which is used to control the stator currents. The reference current amplitude I_{p1} is derived from a binary subtraction of the two rotor positions.

A simplified block diagram of the master-slave interconnection is shown in Fig. 6-2. Here, the difference between the local position and the received position are multiplied by a gain (stiffness) constant K. The inputs, I_{p1} and I_{p2}, control the electromagnetic torque.

The tradeoff for using the amplitude-modulated control method is the increase in complexity of the hardware implementation. Referring to Fig. 6-2, there is an internal feedback of θ_{r1} within the master control system in addition to the external feedback. The control that derives the amplitude of the stator currents adds an additional component to the system.

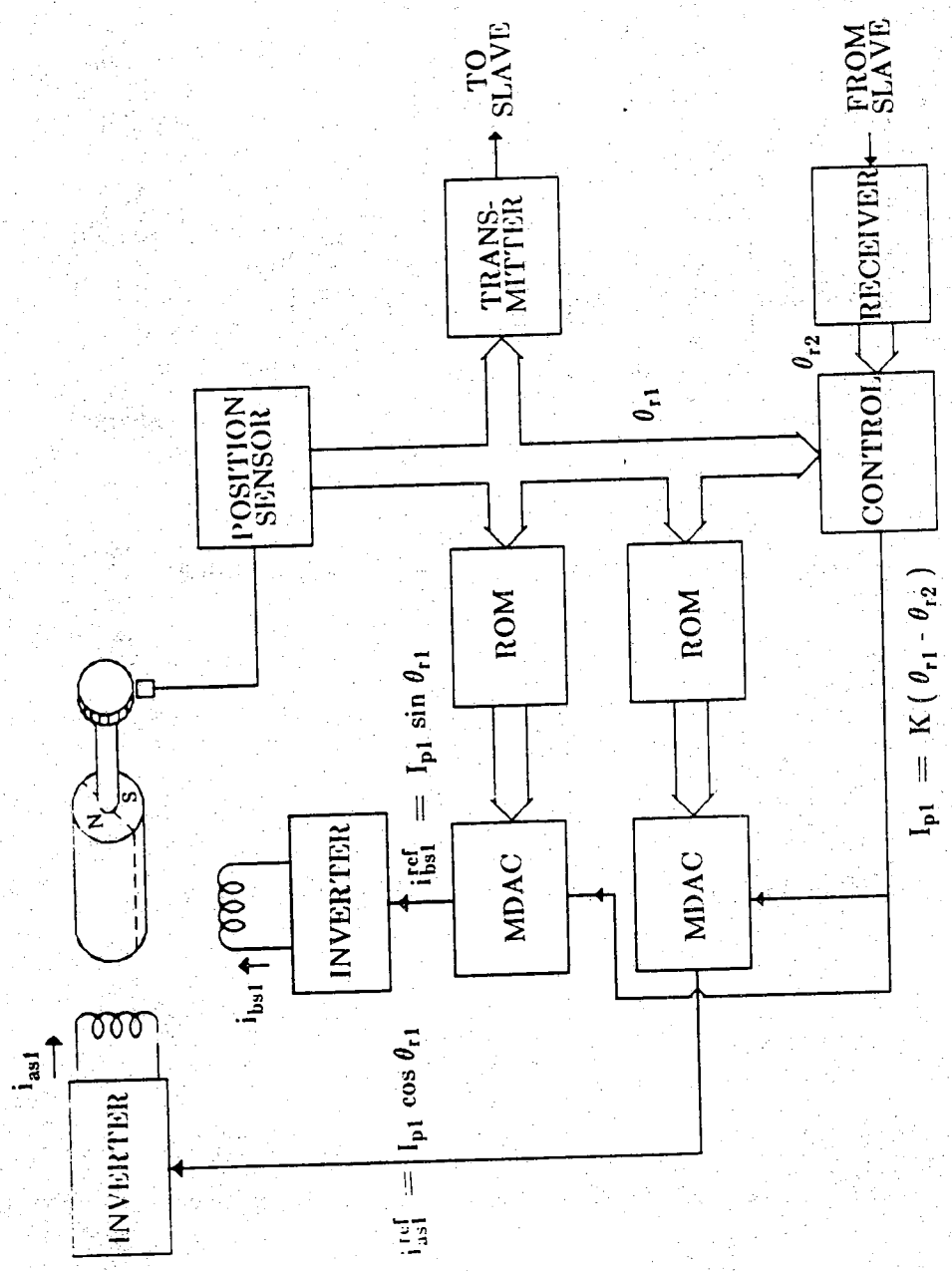

Fig. 6-1 Amplitude-modulated system level control.

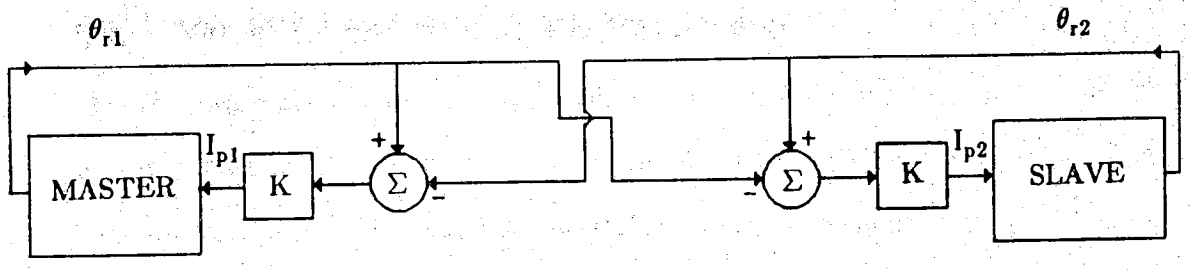

Fig. 6-2 Master-slave interconnections for amplitude-modulated control.

6.4 Computer Analysis of Angle Step Change

A computer study is performed to compare the response of the amplitude-modulated control method of the constant-current control of the previous chapter. The response of the electrical system to a step change in position is shown in Fig. 6-3. All of the assumptions considered in Section 5.4 are assumed to apply here and the same variables are plotted.

Mechanically, the response in Fig. 6-3 is similar to that of the previous study shown in Fig. 5-2. As before, θ_{r1} and θ_{r2} start at the zero position. When the master position θ_{r1} is stepped to 60°, θ_{r2} follows with an initial peak value of 120°. There is an oscillation in θ_{r2} which decays toward 60°. Again, the time-constant associated with the decay of the oscillations of θ_{r2} is approximately 0.73 s and the frequency of these oscillations is close to 278 rad/s.

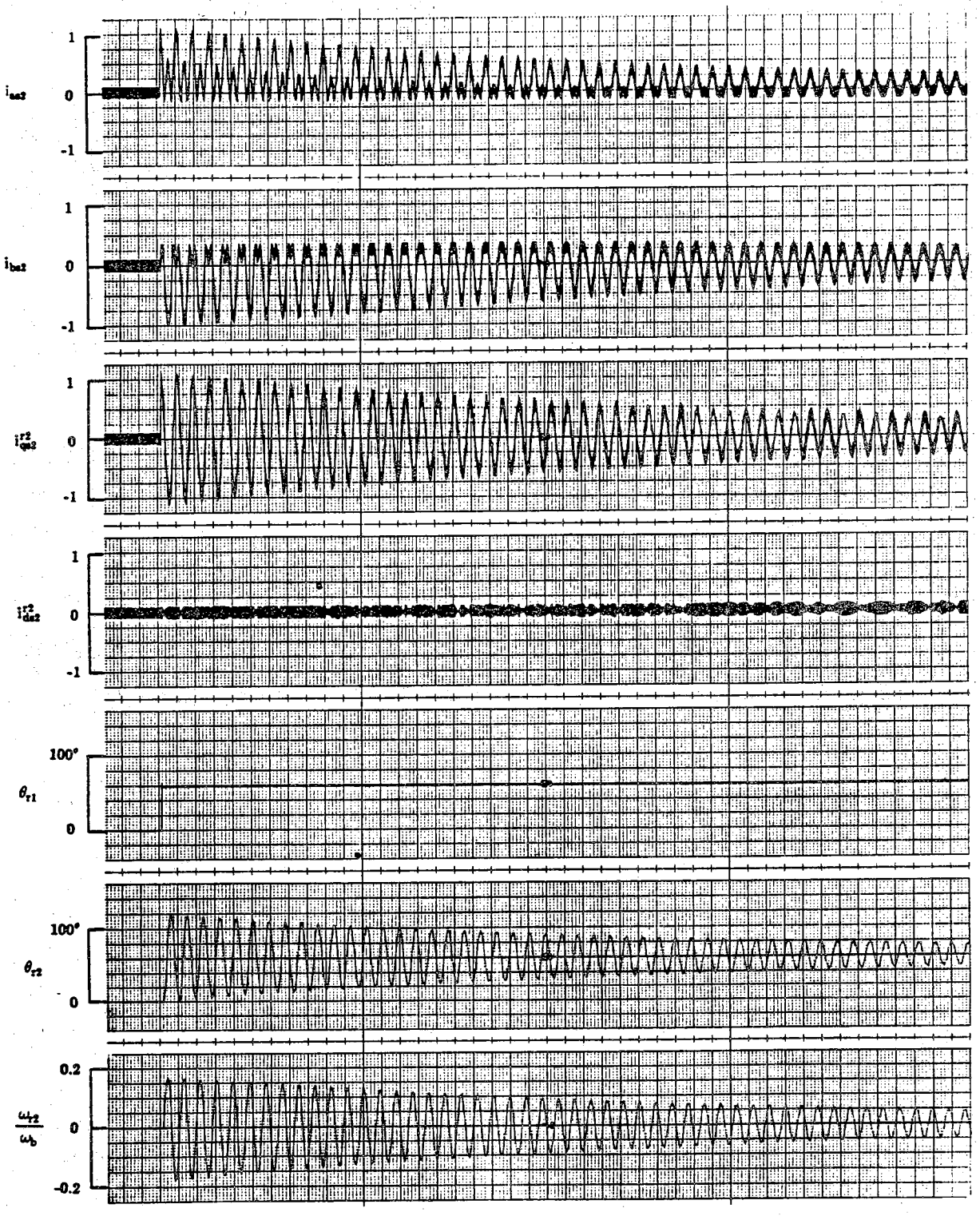

Fig. 6-3 Slave unit response for step change in master position.

The differences in response between the two studies are found in the currents. Prior to the step change in position input, the stator currents are zero. In addition, the stator currents decay back to zero after the step is applied. The stator currents i_{as2} and i_{bs2} are functions of θ_{r2}, and thus they are time varying. i_{as2} peaks when θ_{r2} is a minimum and it has a secondary peak when θ_{r2} is a maximum. The minimum value of i_{bs2} occurs when θ_{r2} is a maximum. i_{qs2}^{r2} oscillates at the same frequency as θ_{r2}, although its response is not sinusoidal. The initial amplitude of i_{qs2}^{r2} is $\pi/3 \simeq 1.05$ pu. This stepping is proportional to the difference between the rotor positions rather than the sine of their differences. As in (6.2.11), i_{ds2}^{r2} remains at small throughout the study.

This alternative method of control offers advantages compared to the original method. The permanent-magnet rotor is not subject to demagnetization because i_{ds}^{r} remains at zero. Also, i_{as2} and i_{bs2} are zero when the rotor is at rest and power is used only when the machine is operated. Although this does not offer an advantage in constant speed applications, considerable power is saved when the teleoperator is used as a positioning device.

The mechanics of this system can easily be confirmed by an eigenvalue analysis. As in (5.4.1), the mechanical relationship in per unit form is,

$$T_{e2} = T_L + 2\,H\,p\,\frac{\omega_{r2}}{\omega_b} + D\,\frac{\omega_{r2}}{\omega_b} \qquad (6.4.1)$$

In this case, the electromagnetic torque is defined in (6.2.15) as

$$T_{e2} = K\,(\theta_{r1} - \theta_{r2}) \qquad (6.4.2)$$

Substituting in T_{e2}, $K = 1$ pu and $T_L = 0$, the mechanical equation becomes

$$(\theta_{r1} - \theta_{r2}) = \frac{2\,H}{\omega_b}\,p^2\theta_{r2} + \frac{D}{\omega_b}\,p\,\theta_{r2} \qquad (6.4.3)$$

Since this differential equation is identical to (5.4.3) and (5.4.4) to (5.4.7), the eigenvalues are the same as those in Section 5.4. Again,

$$\tau = 0.8 \qquad \omega_n = 283.5 \text{ rad/s} \qquad (6.4.4)$$

The above exponential decay time constant τ and the natural frequency of oscillation ω_n matches the results of the computer simulation depicted in Fig. 6-3.

6.5 Computer Analysis of Step Load Torque Input

Although the merits of the teleoperator when used as a positioning device have been shown in Sections 5.4 and 6.4, it is necessary to show its response as a constant speed device. It must be proved that the slave motor will not slip as the master increases speed. The rise-time and the oscillations of the system must be considered. Even though the amplitude-modulated control system in Chapter 6 is considered in this case, the constant-current control method gives identical results.

To analyze the teleoperator's response to a unit step in load torque input, a computer simulation is performed. The study is shown in Fig. 6-4. The following variables are plotted for both the master and the slave: the as-winding stator currents (i_{as1} and i_{as2}), the rotor reference frame currents (i_{qs1}^{r1} and i_{qs2}^{r2}) and the rotor speeds (ω_{r1}/ω_b and ω_{r2}/ω_b) as well the peak current I_{p2}.

In Fig. 6-4, the rotor speeds of ω_{r1}/ω_b and ω_{r2}/ω_b have identical responses except for a negligible delay. Each rotor speed is underdamped and increases to approximately 90% of rated speed with minor oscillations. The teleoperator does not reach rated speed because of the 5% damping loss from each rotor. The amplitude of the stator currents I_{p2} approaches 90% of unity and its oscillation has the same frequency as ω_{r1}/ω_b and ω_{r2}/ω_2. Since the q-axis currents i_{qs1}^{r1} and i_{qs2}^{r2} are functions of I_{p2}, their waveforms are similar to that of I_{p2}. The stator currents i_{as1} and i_{as2} are functions of both I_{p2} and the cosine of the rotor position, so i_{as1} and i_{bs1} vary erratically after the step change. As the amplitude I_{p2} becomes constant, the stator currents become sinusoids. The dominant frequency of oscillation for the stator current amplitude, rotor speeds, and q-axis currents is approximately $\omega_n \simeq 370$ rad/sec. The time-constant of the decay of these oscillations is found to be $\tau \simeq 36$ ms.

A torsional dynamical model can be used to analyze the system response for a step change in the input load torque [8]. In this analysis, the electrical teleoperator system is modeled as if the two rotors were connected by a shaft. The basic set of equations for the mechanical system can be expressed symbolically as

$$T = \frac{2}{\omega_b} H p \bar{\omega} + D \bar{\omega} + \frac{1}{p} K \bar{\omega} \qquad (6.5.1)$$

or in matrix form

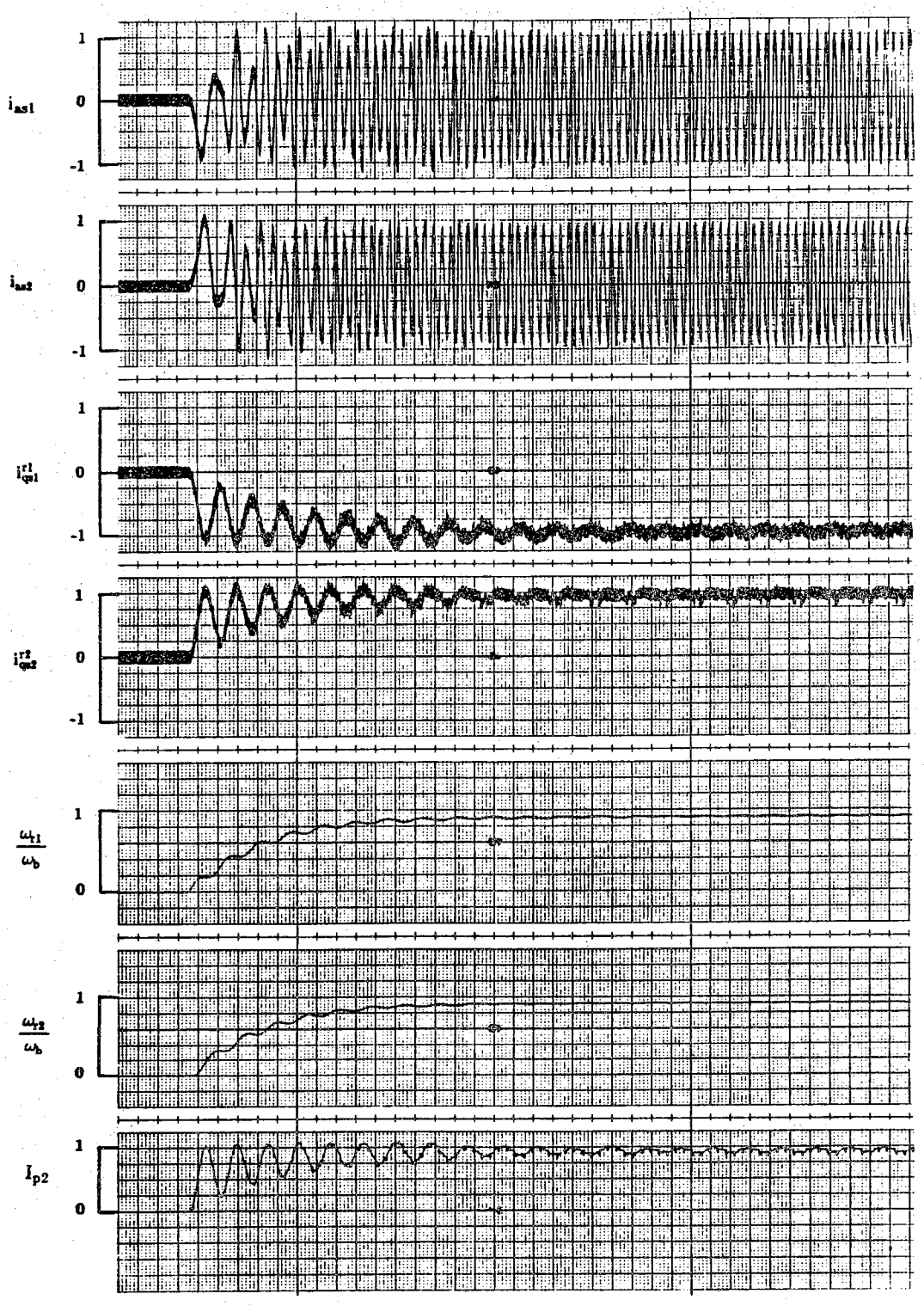

Fig. 6-4 System response for step change in input torque.

$$\begin{bmatrix} T_1 \\ T_2 \end{bmatrix} = p \frac{2}{\omega_b} \begin{bmatrix} H_1 & 0 \\ 0 & H_2 \end{bmatrix} \begin{bmatrix} \omega_{r1} \\ \omega_{r2} \end{bmatrix} + \begin{bmatrix} D_1 & 0 \\ 0 & D_2 \end{bmatrix} \begin{bmatrix} \omega_{r1} \\ \omega_{r2} \end{bmatrix} + \frac{1}{p} \begin{bmatrix} K & -K \\ -K & K \end{bmatrix} \begin{bmatrix} \omega_{r1} \\ \omega_{r2} \end{bmatrix} \tag{6.5.2}$$

Setting T_1 and T_2 to zero and converting to state-equation form results in

$$p \begin{bmatrix} \theta_{r1} \\ \theta_{r2} \\ \omega_{r1} \\ \omega_{r2} \end{bmatrix} = \begin{bmatrix} 0 & I \\ -\frac{\omega_b}{2} H^{-1} K & -\frac{H^{-1}}{2} D \end{bmatrix} \begin{bmatrix} \theta_{r1} \\ \theta_{r2} \\ \omega_{r1} \\ \omega_{r2} \end{bmatrix} \tag{6.5.3}$$

The load torque in the slave is modeled as an additional damping component which is added to the D_2 term. Since identical machines have been assumed in the previous discussions, the inertia H is the same for both the master and the slave. Given that $D_1 = 0.05$ pu, $D_2 = 1.05$ pu and that the machine parameters are the same as the previous studies, the state-equations can now be defined as

$$p \begin{bmatrix} \theta_{r1} \\ \theta_{r2} \\ \omega_{r1} \\ \omega_{r2} \end{bmatrix} = \begin{bmatrix} 0 & 0 & 1 & 0 \\ 0 & 0 & 0 & 1 \\ -80400 & 80400 & -2.5 & 0 \\ 80400 & -80400 & 0 & -52.5 \end{bmatrix} \begin{bmatrix} \theta_{r1} \\ \theta_{r2} \\ \omega_{r1} \\ \omega_{r2} \end{bmatrix} \tag{6.5.4}$$

The eigenvalues of the system are found to be

$$\lambda_1 = -27.61, \quad \lambda_2 = 0 \tag{6.5.5}$$

$$\lambda_3 = -13.70 + j400.0, \quad \lambda_4 = -13.70 - j400.0$$

The results of the eigenvalue analysis are in agreement with the computer results of Fig. 6-4. Since the time-constant associated with the decay of the

natural frequency is the reciprocal of the magnitude of the real part of an eigenvalue, the time-constant associated with λ_1 is $\tau_1 = 36.2$ ms. This is the dominant time-constant observed in Fig. 6-4. The imaginary part of λ_3 and λ_4 correspond to the frequency of oscillation, that is $\omega_n = 400$ rad/s. This frequency is in agreement with the results of the computer simulation.

CHAPTER 7

SUMMARY AND CONCLUSIONS

In this thesis, a brushless dc control system for synchro drives and teleoperator operation has been developed. A mathematical model of the brushless dc actuator and its associated dc-to-ac inverter were first derived. This drive system was then analyzed, with the aid of a computer simulation, to determine its operating characteristics. The speed range in which the torque of the brushless dc machine can be controlled with negligible time delay was determined analytically.

Two control strategies were then proposed to drive the teleoperator system. In the first method, referred to as the constant-current control method, the stator currents were constant-amplitude sinusoidal functions of the rotor positions. An aligning electromagnetic torque was produced which was proportional to the sine of the difference between the two rotor positions. In the second method, referred to as the amplitude-modulated control method, the amplitude of the stator currents were varied as a function of the difference between the two rotor positions.

Computer studies for applications in positioning and variable-speed driving were simulated and analyzed. It was found that both systems had

satisfactory mechanical response characteristics which could be predicted by linear coupled differential equations. The constant-current control method was found to be more desirable when hardware costs are emphasized. The amplitude-modulated control method has the advantages that the permanent-magnet brushless dc motor consumes less power in positioning applications and that the risk of rotor demagnetization is reduced. Both methods were shown to have characteristics which make them advantageous over conventional ac and dc synchro systems.

LIST OF REFERENCES

LIST OF REFERENCES

[1] Benjamin C. Kuo, *Automatic Control Systems,* Prentice-Hall, 1987.

[2] William A. Wolovich, *Robotics: Basic Analysis and Design,* Holt, Rinehart and Winston, 1987.

[3] A.E. Fitzgerald, C. Kingsley, S. Umans, *Electric Machinery,* McGraw Hill, 1983.

[4] Paul C. Krause, *Analysis of Electric Machinery,* McGraw Hill, 1986.

[5] A.B. Plunkett, "A Current-Controlled PWM Transistor Inverter Drive," Conf. Rec. IEEE/IAS Annual Meeting, pp. 786-792, Oct. 1979.

[6] B.K. Bose, *Power Electronics and AC Drives,* Prentice-Hall, 1986.

[7] P.M. Lin, Lumped System Theory - Class Notes, Purdue University, 1988.

[8] Oleg Wasynczuk, Torsional Dynamics - Class Notes, Purdue University, 1986.